Facies (2005) 51: 460–479
DOI 10.1007/s10347-005-0061-x

ORIGINAL ARTICLE

Thomas Hornung · Rainer Brandner

Biochronostratigraphy of the Reingraben Turnover (Hallstatt Facies Belt): Local black shale events controlled by regional tectonics, climatic change and plate tectonics

Received: 8 November 2005 / Accepted: 10 March 2005 / Published online: 10 June 2005

Abstract For the first time, two outcrops near Bad Dürrnberg (2 km SSW Hallein, Austria) allowed for a continuous multistratigraphical investigation of the Reingraben Turnover in the Hallstatt facies belt. After a phase of reefal sedimentation during the Julian 1 (Early Carnian), a sudden increase in terrigenous input (Reingraben Turnover) caused the breakdown of the carbonate factory at the beginning of the Julian 2 (late Early Carnian). In starved basins produced by syndepositional tectonism, black shales locally accumulated. Stable isotopes of oxygen and carbon do not suggest a change in seawater chemistry during the turnover. Shallow-water carbonate production resumed slowly during the Tuvalian (Late Carnian), and complete recovery was finished near the Carnian-Norian transition. Because similar events are recorded globally, climatic changes (monsoonal circulation) controlled by plate tectonics are favoured as triggers of the event.

Based on lithology and microfacies, detailed sampling, and analysis of conodont faunas and the resulting detailed conodont zonation enabled us to establish the duration of the Reingraben Turnover (Julian 1/IIc to Julian 2/II).

Keywords Carnian · Tethys · Northern Calcareous Alps · Multistratigraphy · Conodonts · Microfacies · Stable isotopes

Introduction

The Reingraben Turnover is one of most conspicuous stratigraphic changes, which is mirrored in all facies belts of the entire NW Tethyan continental margin (Schlager and Schöllnberger 1974). This turnover is reflected in the biofacies and lithofacies as well as by evolutionary events. The development of widespread, prograding carbonate platforms was suddenly interrupted by siliciclastic input. Furthermore, several factors indicate an almost complete breakdown of reef ecosystems, combined with an abrupt decline of carbonate production (e.g., Riedel 1991; Rüffer and Zamparelli 1997; Flügel and Senowbari-Daryan 2000; Keim et al. 2001). Despite many investigations, the causes of the turnover remain poorly documented. In the present paper, global climatic changes combined with plate tectonics are supposed as the main driving force.

Many authors (e.g., Angermeier et al. 1963; Jerz 1966; Schuler 1968; Schulz 1970; Grottenthaler 1978) document marginal-marine facies at the northern alpine Raibl Event (= Reingraben Turnover in the Northern Alps), although these successions, deposited in high-energy conditions, most probably gained significant sedimentary gaps. Also, the basinal successions (Hallstatt facies) of the Eastern Alps had caught the attention of many authors (e.g., Plöchinger 1955, 1976, 1983, 1984, 1996; Mandl 1984, 1999; Gawlick 2000). Present descriptions have been kept also brief (e.g., Gawlick et al. 1999a), although the potential of complete basinal sequences (low-energetic setting) ought to be much higher than in the shallow-water facies.

Gawlick et al. (1999a) mentioned the Freygutweg section (within recent road cuttings), and the disused Jakobberg gallery which contain Reingraben (= *Halobia*) Shales and, therefore, represent the Reingraben Turnover mentioned above. As a pilot study in the context of FWF-Project P 16878 "The Carnian Turnover in the Western Tethyan Realm", these sedimentary successions were examined from a multistratigraphical viewpoint with the goal to establish a high-resolution succession representative of the Hallstatt area.

Geography, palaeogeography and stratigraphy

Geography

Both sections are located near Bad Dürrnberg, about 2 km SSW of Hallein (Fig. 1). This area is flanked by the N-S striking Hoher Göll and Rossfeld mountain range

T. Hornung (✉) · R. Brandner
Institute of Geology and Palaeontology, University of Innsbruck,
Innrain 52,
6020 Innsbruck, Austria
e-mail: thomas.hornung@uibk.ac.at

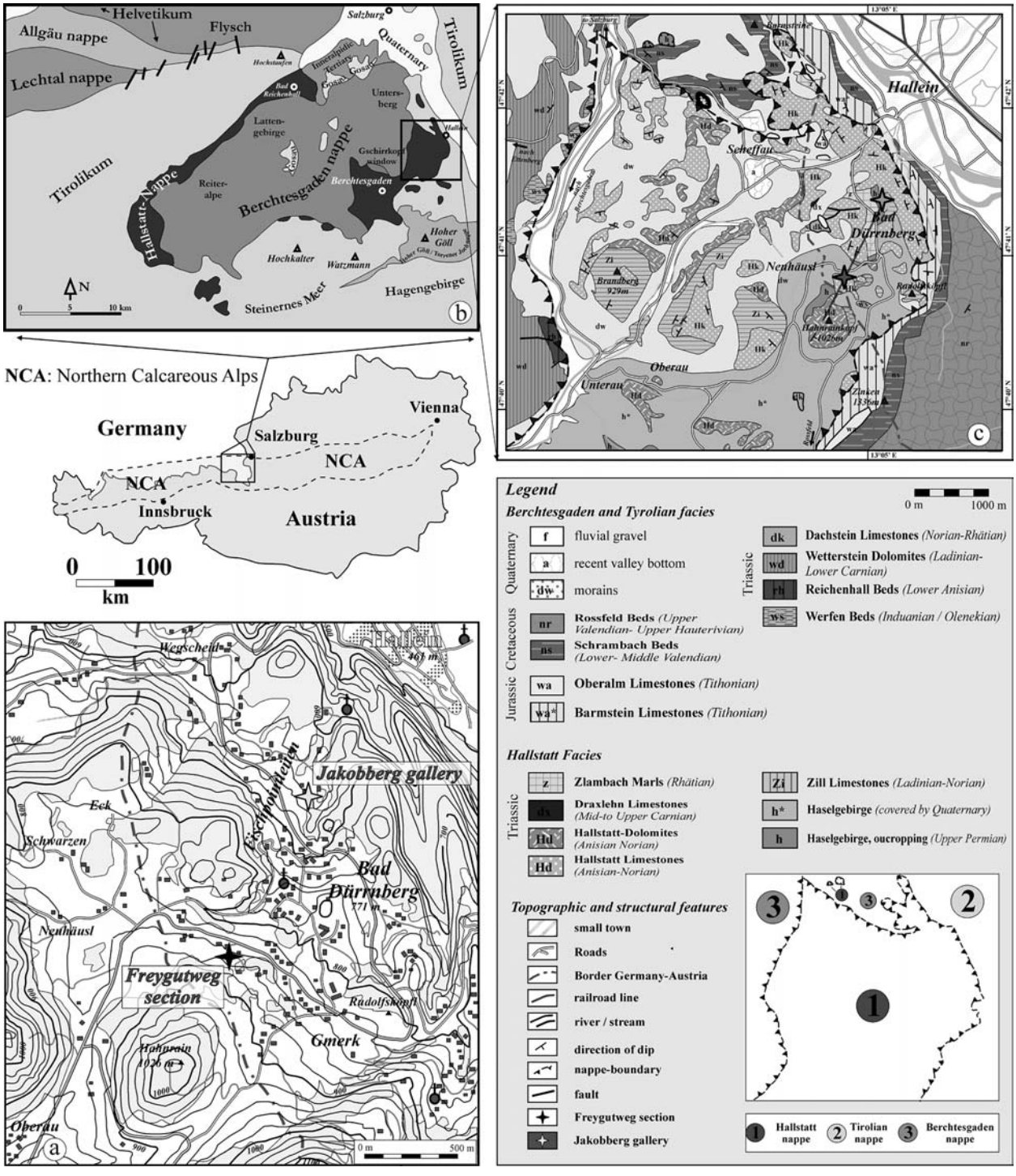

Fig. 1 **a** Geographic position of the sections and **b** the main geological and tectonical settings of the area (left column—modified after Braun 1998). **c** Simplified geological map of the fault-block region of Hallein-Berchtesgaden (right column—modified after Plöchinger 1955, Prey 1969, and Gawlick 2000)

near Salzburg, and by a glacially cut escarpment towards Berchtesgaden (Fig. 1).

Palaeogeography

The Reingraben Turnover occurred during a rearrangement of tectonic plates: the Cimmerian Micro-Continent, positioned at the northern margin of the Tethyan realm, collided with the Eurasian plate as the supercontinent Pangaea disintegrated during the formation of the Neotethys and the future central Atlantic Ocean (Fig. 2a). Near the Ladinian-Carnian boundary, the northwestern part of the Tethys was split into separate oceanic basins (Stampfli and Borel 2002; see Fig. 2): the subducted Palaeo-Tethys in the south, and

the Hallstatt-Meliata Ocean in the north. The investigated area is situated at the northwestern margin of the Hallstatt-Meliata Ocean (Fig. 2).

After a phase of rapid Middle Triassic rifting, the Wetterstein shelf area shallowed due to a significant decrease in tectonic subsidence (Brandner 1984). This induced a change in carbonate platform geometries. In the earliest Carnian, a phase of Ladinian platform aggradation abruptly changed to a marked progradation.

During the Early to Late Carnian, several main facies areas developed on the shallow and hemipelagic epicontinental shelf of the NW Tethys. They include, from present NW to SE, the terrigenous Keuper facies belt of present Germany, and the laterally adjacent shelf facies of the so-called Bajuvaric and Tirolic tectonostratigraphic units of the Eastern Alps (Fig. 2b). The area of Bajuvaric and Tirolic units can be subdivided into different facies belts: a) a northern carbonate platform (Wetterstein Formation) interfingered towards the southeast with the, b) intraplatform-basinal Reifling Formation. Towards the southeast, within the Tirolikum, another up to 2000 m thick carbonate platform of the Wetterstein-Formation is marking the shelf margin area. The toe of the slope interfingers with Reifling Beds, and c) the Hallstatt facies belt. These regions can be

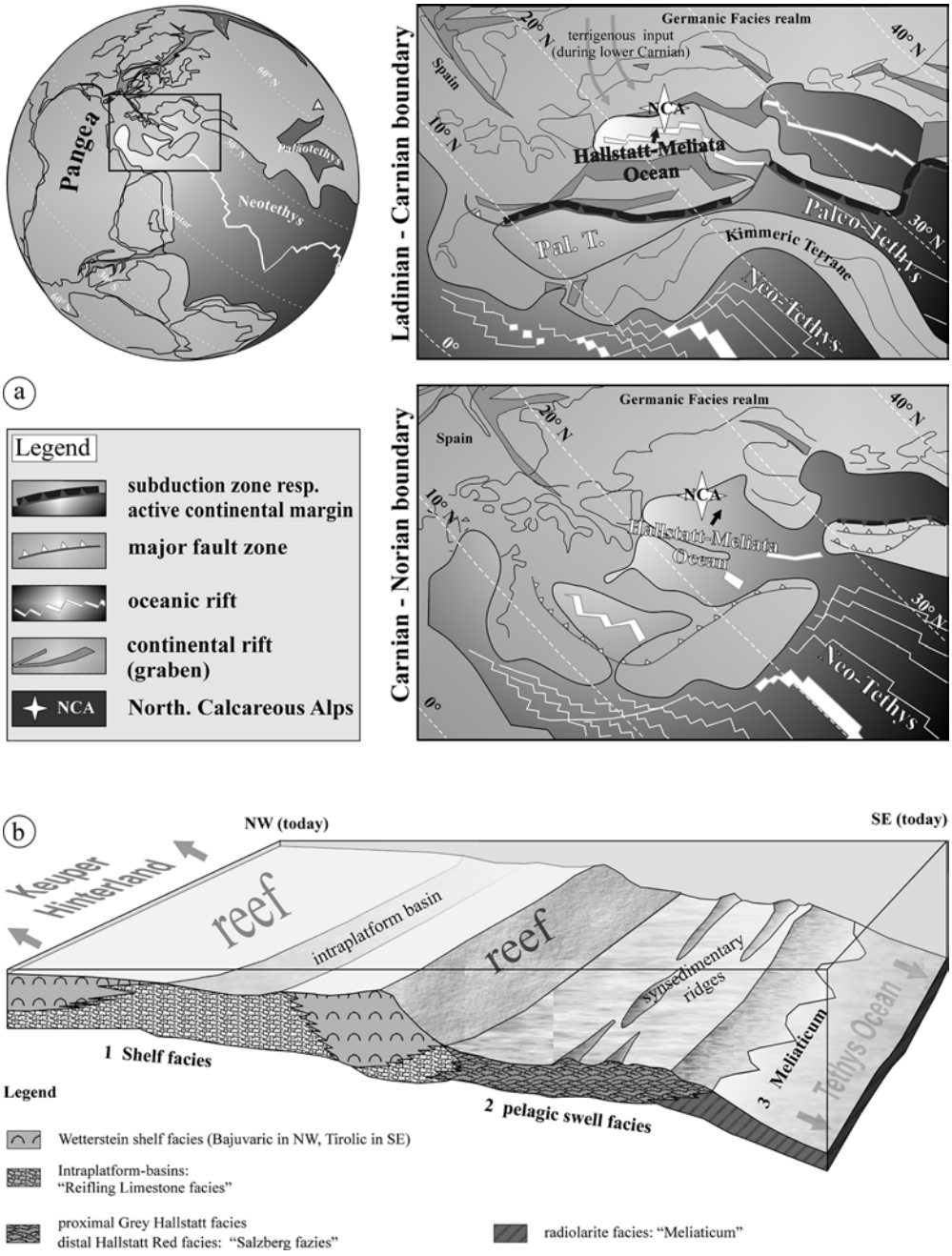

Fig. 2 **a** Global palaeogeographic situation during Carnian and Norian times (modified after Stampfli and Borel 2002), and a generalised, ideal facies model (**b**) for the northwestern Tethyan margin (Carnian). Exaggerated relief

subdivided in a proximal Hallstatt Grey facies and a more distal Red Hallstatt facies belt ("Salzberg facies"; see also Fig. 2b).

Due to tectonic shortening, lateral displacement, and subsequent erosion, the Meliaticum (see Fig. 2b), deposited on oceanic crust, is preserved only in local tectonic slivers (e.g., Mandl and Ondrejickova 1993).

Around the Julian 1/Julian 2 boundary, large rivers transported high amounts of siliciclastics in a bypass-system from the Baltic Craton towards Central Europe and, finally, towards the continental margin of the Hallstatt-Meliata Ocean (Tollmann 1976; Aigner and Bachmann 1992). The terrigenous material accumulated in basinal areas and, subsequently, also on the shelves. This interrupted the reefal development and resulted in a distinct lithological turnover (Reingraben Turnover). As shown herein, the shallow-water carbonate factory was shut off throughout the Tuvalian and resumed during the Early Norian.

Already in the Middle and Upper Triassic, salt diapirism, initiated by the Permian Haselgebirge, resulted in synsedimentary motions, documented by numerous sediment-filled fissures (Schlager 1969). The Jurassic transtensional Penninic ocean basin caused the separation of the Austroalpine facies belt, including the NCA, from the European hinterland. Coevally, compressional movements in the western Tethys and on Austroalpine shelves resulted in the development of a nappe stacking (Mandl 1999), which is well preserved in the Hallein-Berchtesgaden region. First, the Tirolic facies belt was overthrusted by the Juvavic (= Hallstatt) nappe (Fig. 1a). Increased transpressive motions during the latest Jurassic and Cretaceous led to an "out of sequence" thrusting of both units (Mandl 1999) producing a doubling of the nappe complex. The "lower" stack was in turn overthrusted by the Berchtesgaden nappe (Fig. 1a; southern Tirolic facies). The overlying (southern) blocks were eroded during the Cretaceous and the remaining relief was sealed by the Tertiary Gosau Group (Fig. 1a). For further discussion see, e.g., Decker et al. (1987), Frank (1987), Neubauer (1994), Schweigl and Neubauer (1997), Gawlick and Lein (1997, 2000), Gawlick et al. (1999b), Gawlick (2000), Gawlick and Diersche (2000), Frisch and Gawlick (2003).

Stratigraphy of the Hallstatt nappe

This unit is characterised by the interfingering of different but isochronous lithologies deposited in several subfacies belts. The primary spatial arrangement of both the proximal Grey facies and the distal Red facies (Fig. 2b) was profoundly overprinted by tectonic shearing and overprinting. The first reconstructing attempt of a standardised Hallstatt stratigraphic succession was published by Schlager (1969), revised by Mandl (1984), and finally specified by Mandl (1999) and Gawlick (2000); see Fig. 3. The primary position of the subfacies belts was up to the amounts of carbonate production on adjacent factories (Reijmer and Everaas 1991) as well as on underground movements. Already in the Upper Triassic, the submarine relief was composed of

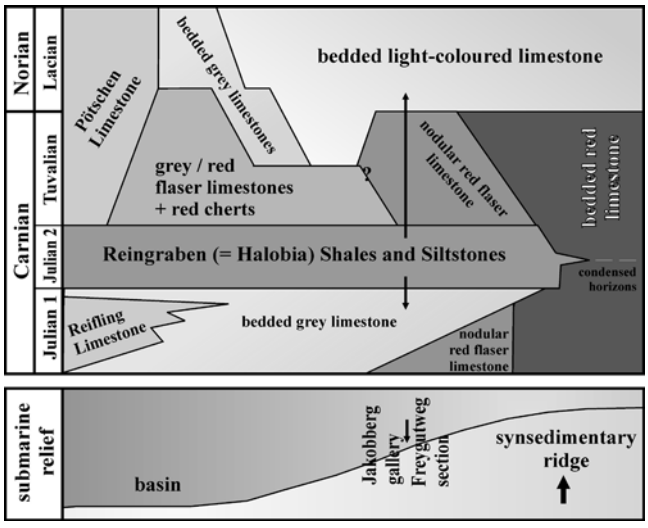

Fig. 3 Stratigraphic succession depending on palaeomorphological patterns (modified after Mandl 1984, 1999 and Gawlick 2000). The position of the sections might be placed on the upper edge between the top of the ridges and the basins (*thin black arrows*)

flat, elongated ridges (synsedimentary diapiric ridges; see Figs. 2b, 3) with calcareous successions and shallow basins inbetween with prevalent marly and clay-rich deposits.

Sections

Freygutweg section

First mentioned and investigated by Gawlick et al. (1999a), this section consists of condensed lowermost Carnian to Middle Lacian rocks. All beds dip uniformly SSE at 25°. The section is overturned. The basal part consists of a 5 m thick-bedded grey limestone sequence, covered by 2.75 m thick grey to violet-coloured Reingraben Shales. These units are overlain by about 2.3 m thick nodular red flaser limestones and 3 m thick medium-bedded light-coloured limestones (see Fig. 4). Unfortunately, the transition between the bedded grey limestones and the Reingraben Shales is completely overgrown and probably tectonically sheared: several excavation-attempts to a depth to circa 1 m reached no solid bedrock.

Jakobberg gallery

The stratigraphic succession ranges from greyish-coloured bedded limestones of the Early Fassanian and Langobardian to the "Liasfleckenmergel" (basal Jurassic; Gawlick and Lein 1997, 2000; Gawlick et al. 1999a).

Medwenitsch (1949, 1958, 1962, 1963) mapped the galleries and notes dark Reingraben Shales intercalated between the overlying monotonous Norian-Rhaetian marl series and the underlying grey-bedded limestones. Gawlick and Lein (1997, 2000) revised the Jakobberg and Wolfdietrich galleries: the part of interest containing the Reingraben Turnover was described only briefly, without any detailed stratigraphic and information about the Carnian succession.

		Stage	Ammonite Zone (Kozur 2003)	Conodont Zone (Tethys) (Kozur 2003)	Ammonite Zone Salzkammergut (Krystyn 1980)	Conodont Ass. Zone Salzkammergut (Krystyn 1980)
Norian	214	Lacian 3	*Juvavites magnus*	*Epigondolella triangularis* *Norigondolella hallstattensis*	*Juvavites magnus*	*E. spatulata* Assemblage Zone
		Lacian 2	*Malayites paulckei*	*Epigondolella quadrata*	*Malayites paulckei*	*E. abneptis* Assemblage Zone
	216	Lacian 1 (216.5)	*Stikinoceras kerri*	*E. ?primitia - M. communisti*	*Guembelites jandianus*	*E. primitia* Assemblage Zone *M. communisti* Assemblage Zone
Carnian		Tuvalian 3	*Klamathites macrolobatus*	*Epigondolella pseudodiebeli*	*Anatropites spinosus*	
	218					*G. nodosa* Assemblage Zone
	220	Tuvalian 2	*Tropites welleri*	*Epigondolella nodosa*	*Tropites subbullatus*	
	222			*Paragondolella carpathica*		*G. polygnathiformis* Assemblage Zone
	224	Tuvalian 1 (225)	*Tropites dilleri*	*P. postinklinata-P. polygnathiformis*	*Tropites dilleri*	
	226	Julian 2	*Austrotrachyceras austriacum* *Trachyceras aonoides*	*Gladigondolella tethydis* *Paragondolella polygnathiformis*	*Trachyceras austriacum* II / I	*Gl. tethydis* Assemblage Zone
		Julian 1 (228)	*Trachyceras aon* *Daxatina canadiensis* *Frankites sutherlandi*	*Budurovignathus diebeli-* *Paragondolella polygnathiformis*	*Trachyceras aonoides* II / I	*C. mostleri* Assemblage Zone
Ladinian	228	Langobardian 3	*Frankites regoledanus*	*Budurovignathus supralongobardica*	*"Sutherlandi"*	
	230	Langobardian 2	*Protrachyceras archelaus*	*Budurovignathus mungoensis*	not reported	not reported
		Langobardian 1 (231.4)	*Protrachyceras gredleri*	*Budurovignathus hungaricus*		
	232	Fassanian 3	*Eoprotrachyceras curionii*	*Budurovignathus truempyi*		
		Fassanian 2	*Nevadites secedensis*	*Paragondolella ?trammeri* *Neogondolella aequidentata*		
	234					

Fig. 4 Comparison of two biostratigraphic zonations. Left columns according to Kozur (2003), the two right columns after Krystyn (1980, 1983) and referring to the Salzkammergut area

Based on bed by bed sampling, the present paper provides detailed biostratigraphic and microfacial information of the basinal Hallstatt facies for the first time. Bedded grey limestones are sharply overlain by thinly-bedded greenish marly limestones (Fig. 5a), subsequently followed by an 1.3 m thick succession of ochre-coloured limestones and marls (Fig. 5b), in turn overlain by about 1.1 m thick black Reingraben Shales. The boundary between bedded grey limestones and green marly limestones (Fig. 5a) as well as ochre coloured-limestones and Reingraben Shales (Fig. 5c),

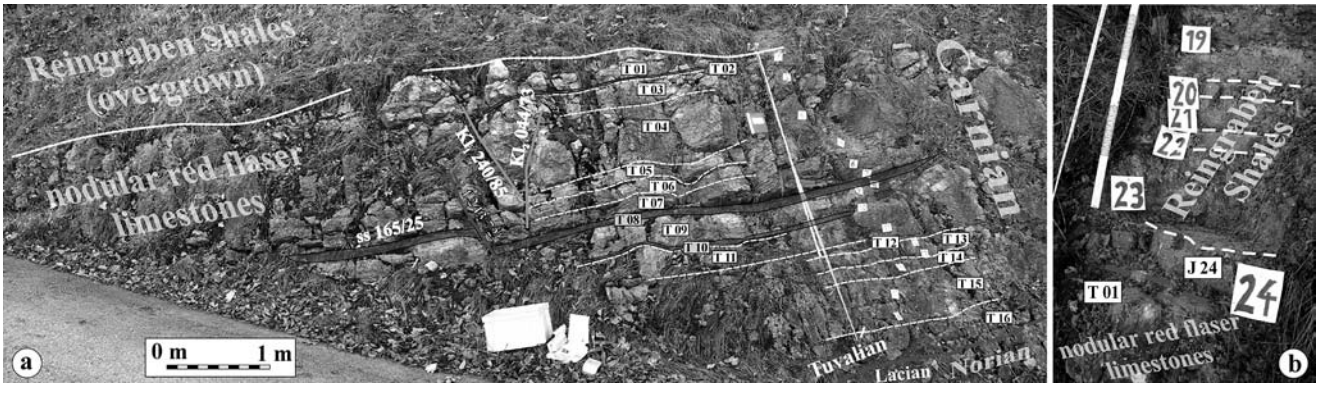

Fig. 5 Upper part of the Freygutweg Section showing (**a**) the nodular red flaser limestones and (**b**) the Reingraben Shales

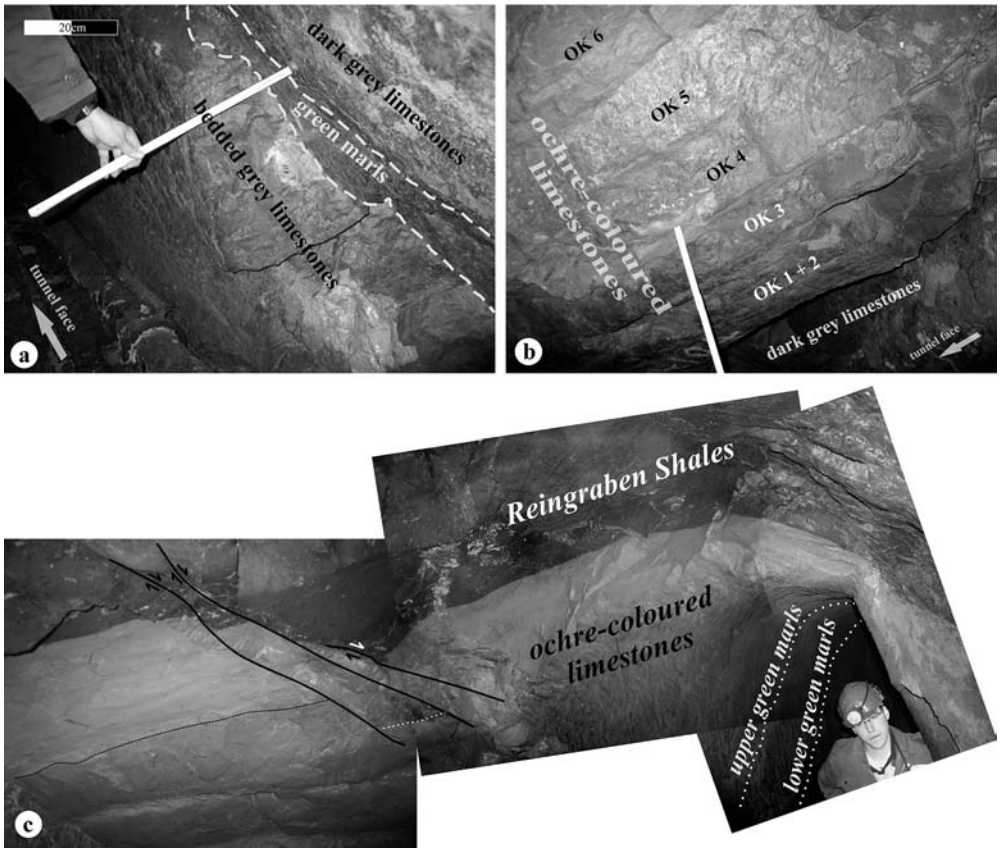

Fig. 6 **a** Sharp and undulating boundaries between the bedded grey limestones and the green marly limestone intercalation. **b** Ochre-coloured limestone succession, alternating with thinly bedded marly intercalations. **c** The sharp transition from ochre-coloured limestones to the black Reingraben Shales demonstrates the drastic change in environmental conditions connected with the "black shale-event"

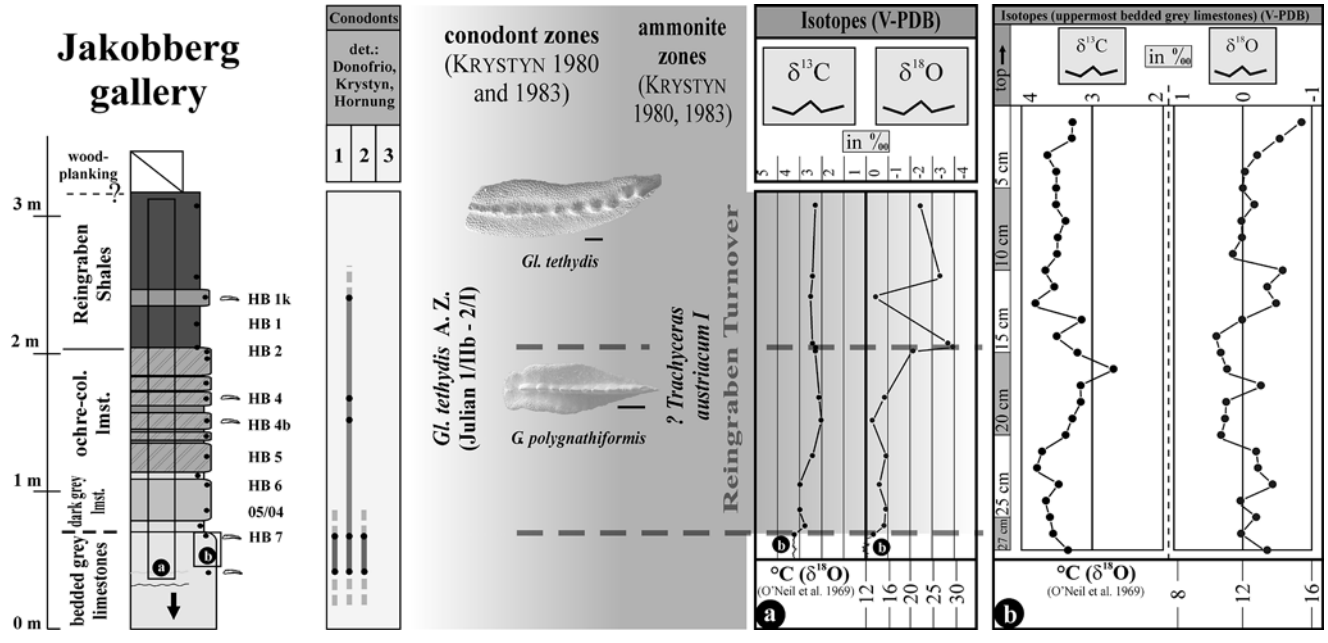

Fig. 7 Lithology, stable isotopes, conodont biostratigraphy and conodont zones (after Krystyn 1980 and 1983) of the Jakobberg gallery. **a** Isotopic sequence of the complete section, **b** detailed isotopic sequence of the uppermost 30 cm of the bedded grey limestones. Palaeotemperatures after O'Neil et al. (1969). Different species in the conodont box: (1) = *Gladigondolella tethydis*; (2) = *Gladigondolella tethydis* ME; (3) = *Gondolella polygnathiformis*

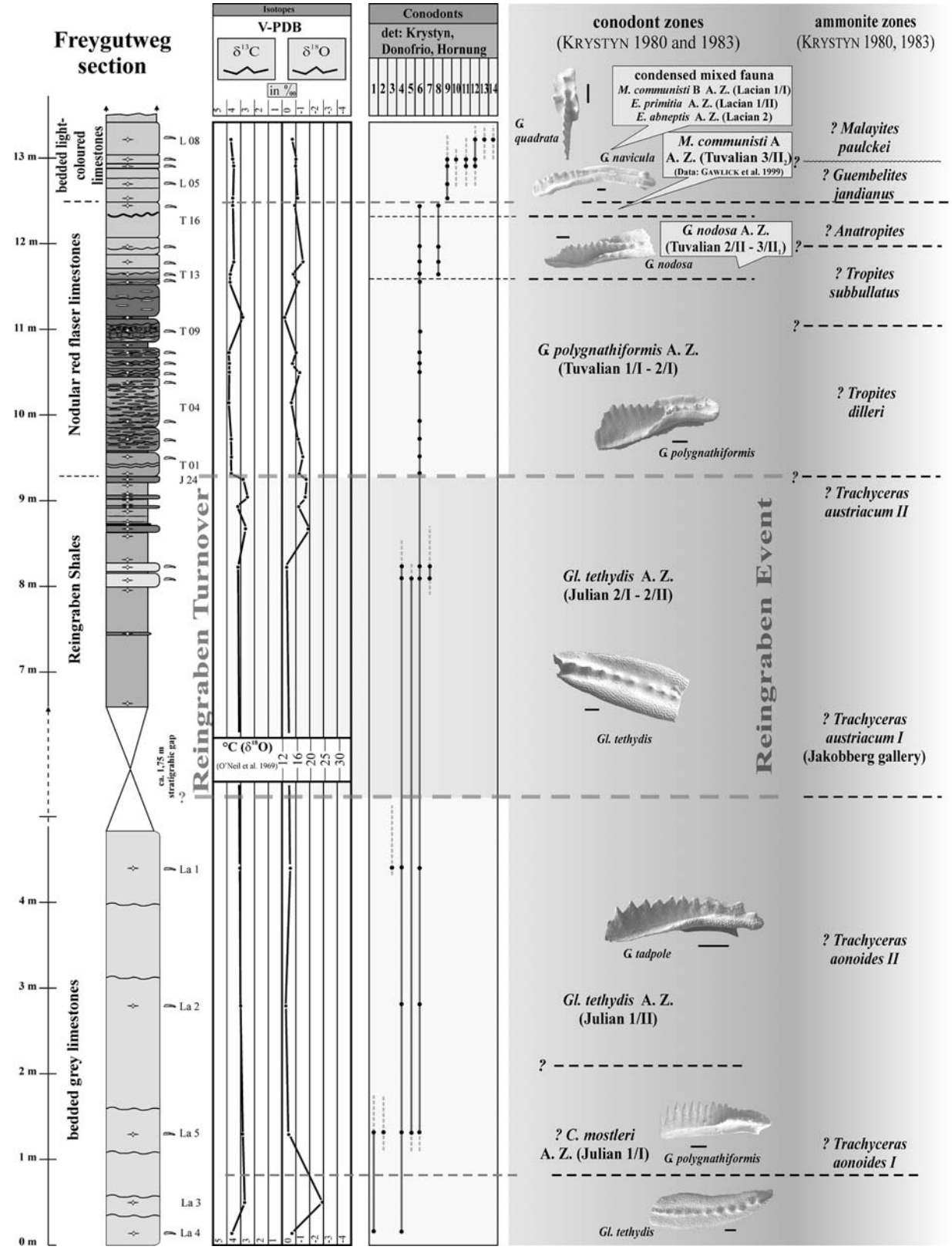

Fig. 8 Lithology, stable isotopes, conodont biostratigraphy, and reconstructed conodont zones (after Krystyn 1980 and 1983) of the Freygutweg section. Due to the lack of ammonites, the ammonite zones are construed after the conodont zones (the exact boundaries are, therefore, questionable). Palaeotemperatures after O'Neil et al. (1969). Different species in the conodont box: (1) = *Enantiognathus petraeviritis*; (2) = *Hindeolella lautissima*; (3) = *Gondolella tadpole*; (4) *Gladigondolella tethydis*; (5) *Hindeolella pectiniformis*; (6) *Gondolella polygnathiformis*; (7) *Hindeolella* sp.; (8) = *Gondolella nodosa*; (9) = *Gondolella navicula*; (10) = *Ozarkodina* sp.; (11) = *Epigondolella triangularis*; (12) = *Epigondolella abneptis*; (13) = *Epigondolella spatulata*; (14) = *Epigondolella quadrata*

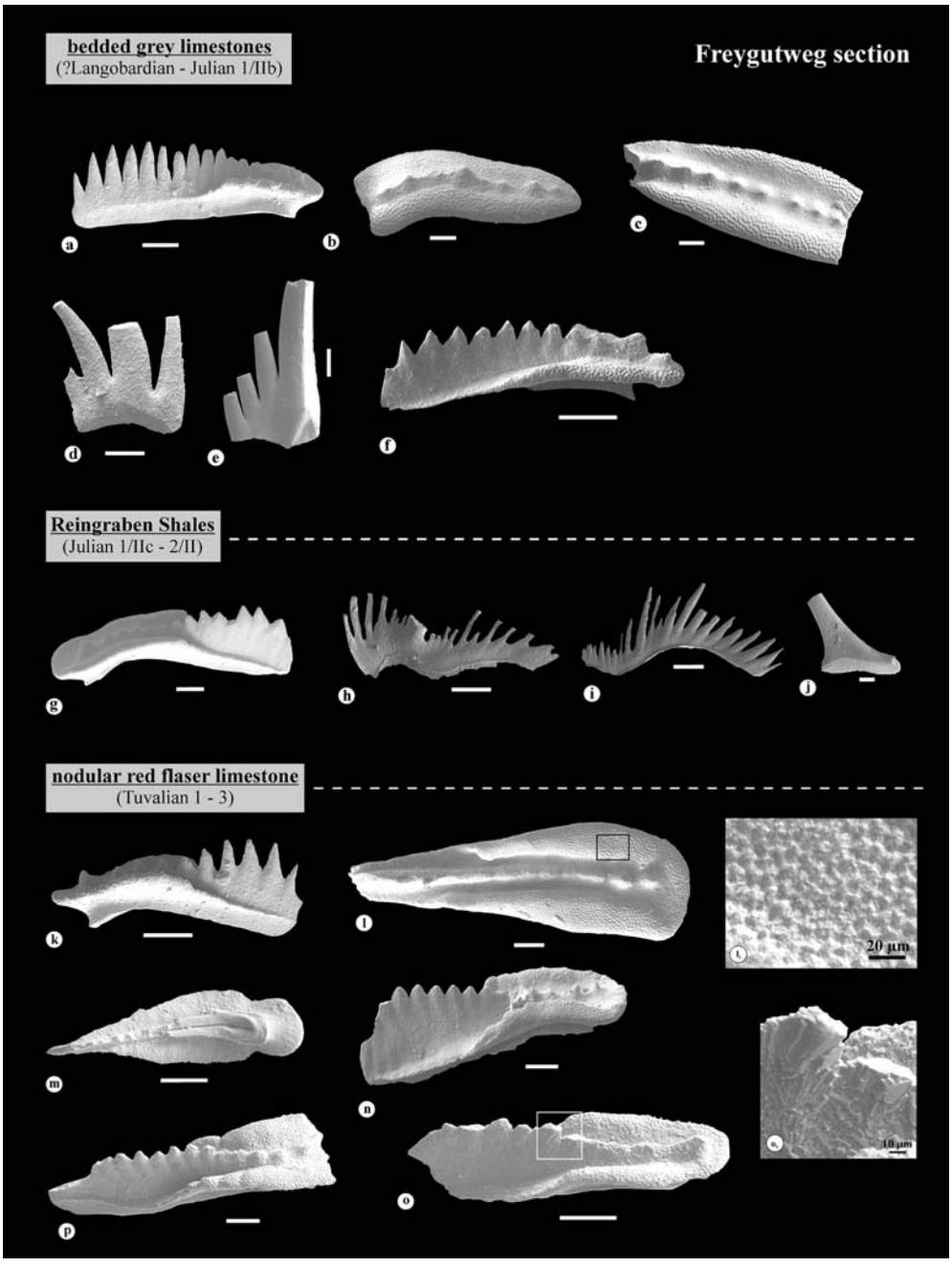

Fig. 9
Conodonts of the Freygutweg section (Lowermost Julian to uppermost Tuvalian); scale bar = 100 µm: **a** *Gondolella polygnathiformis*, Budurov and Stefanov; La 5; CAI = 1.0–1.5; **b** *Gladigondolella tethydis*, Huckriede; La 4; CAI 1.0–1.5; **c** *Gladigondolella tethydis*; La 2; CAI 1.0–1.5; **d** *Enantiogratus petraeviritis*, Huckriede; La 4; CAI 1.0–1.5; **e** *Hibbardella lautissima*, Huckriede; La 5; CAI 1.0–1.5; **f** *Gondolella tadpole*, Hayashi; La 2; CAI 1.0–1.5; **g** *Gondolella polygnathiformis*; J 16a; CAI 1.0; **h** *Hindeolella pectiniformis*, Huckriede; J 16a; CAI 1.0; **i** *Hindeolella pectiniformis*; J 16a; CAI 1.0; **j** *Gladigondolella tethydis* ME, Huckriede; J 16b; CAI = 1.0; **k** *Gondolella polygnathiformis*; T 01; CAI = 1.0; **l** *Gondolella polygnathiformis*; T 04; CAI = 1.0; l_1) *Gondolella polygnathiformis*; detail from **l**; **m** *Gondolella polygnathiformis*; T 06; CAI = 1.0; **n** *Gondolella polygnathiformis*; T 12; CAI = 1.0; **o** *Gondolella polygnathiformis*; T 13; CAI = 1.0; o_1 *Gondolella polygnathiformis*; detail from **o**; **p** *Gondolella nodosa*, Hayashi; T 13, CAI = 1.0

respectively, mark two distinctive lithological changes. Both "events" are conformable and were not caused by tectonic overprinting.

Whereas the lower boundary of the Reingraben Shales is exposed, the upper boundary to overlying nodular red flaser limestones is walled by wood planking and/or sheared. All layers dip at 60° to SSE and in addition are displaced by normal faults dipping northward at 45° (Fig. 5c).

Biochronostratigraphy

The first chronostratigraphic charts for the Salzkammergut region, based on ammonites and conodonts were published by Krystyn (1970) and revised several times (Krystyn 1973, 1980, 1983). At present, global ammonite and conodont biochronology distinguish between several bioprovinces. The Tethyan bioprovince was compiled and constructed mainly by Gallet et al. (1994) and revised by Krystyn et al. (2002). This study focuses on the regional results of Krystyn (1980, 1983; see also Fig. 6).

Fortunately, almost all the limestone beds contained enough conodonts to carry out biostratigraphic zonation and to determine the timeframe of the Reingraben Turnover. Further examinations (in the framework of the FWF-Project P 16878) on other globally distributed sections in different main facies belts will eventually call for a revision or a refinement of the present results (Figs. 7 and 8).

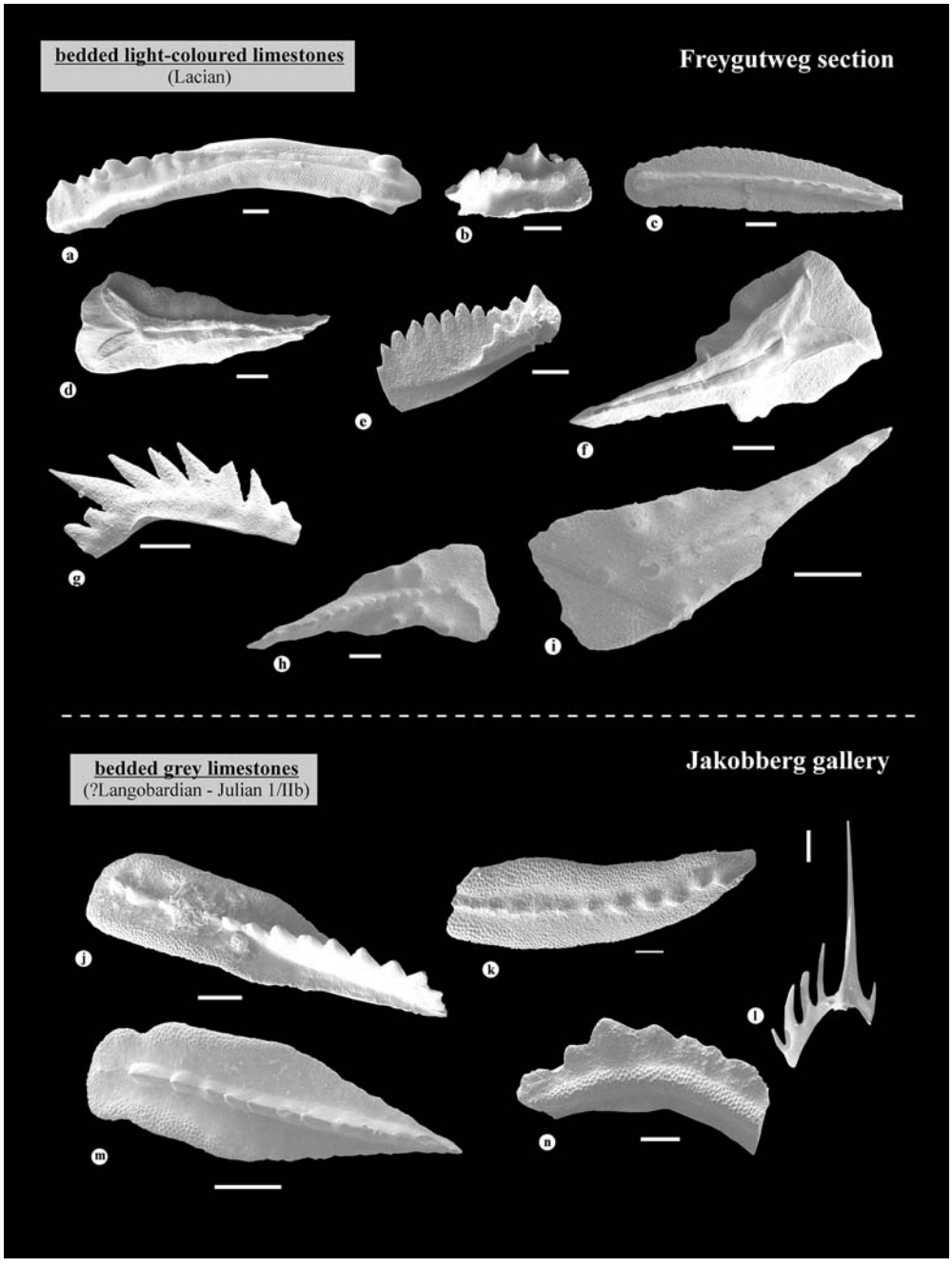

Fig. 10 Conodonts of the Freygutweg section and Jakobberg gallery; scale bar = 100 μm: Conodonts of the Freygutweg section (Early and Middle Norian): **a** *Gondolella navicula*, Huckriede; L 06; CAI = 1.0; **b** *Epigondolella abneptis* s.l., Huckriede; L 06; CAI = 1.0; **c** *Gondolella navicula*; L 07; CAI = 1.0; **d** *Epigondolella cf. triangularis*, Budurov; L 07; CAI = 1.0; **e** *Epigondolella abneptis*, Huckriede; L 07; CAI = 1.0; **f** *Epigondolella spatulata*, Huckriede; L 08; CAI = 1.0; **g** *Ozarkodina sp.*; L 08; CAI = 1.0; **h** *Epigondolella quadrata*, Huckriede; L 07; CAI = 1.0; **i** *Epigondolella quadrata*; L 08; CAI = 1.0. Jakobberg gallery: Top of bedded grey limestones: **j** *Gondolella polygnathiformis*, Budurov and Stefanov; HB 7; CAI <1.0; **k** *Gladigondolella tethydis*, Huckriede; HB 7; CAI <1.0; **l** *Didymodella alternata*, Mosher; HB 7; CAI <1.0; **m** *Gondolella polygnathiformis*; HB 7; CAI <1.0; **n** *Gladigondolella tethydis*; HB 7, CAI <1.0

Excluding the bedded grey limestones, the lithological succession differs within both sections. The Reingraben Shales, which would allow for the correlation of both sections, exhibit stratigraphic gaps. The lower boundary, which is exposed in the Jakobberg gallery, might be tectonically sheared in the Freygutweg section; the upper boundary, exposed at the Freygutweg, is not preserved in the Jakobberg gallery. Intercalated thin-bedded calcareous beds in upper parts of the Reingraben Shales, which would enable further correlations, were not mentioned by former authors. Furthermore, the Reingraben Shales preferentially acted as a shear plane (e.g., Schweigl and Neubauer 1997) resulting in very rare outcrops of the shales in the Hallstatt Red facies. Due to this, a correlation of both sections should

not be attempted using only lithological and facies criteria, but rather with biostratigraphic evidence (Figs. 7 and 8).

The first occurrence of *G. polygnathiformis* Budurov and Stefanov (Fig. 9a) places the Ladinian-Carnian boundary at the base of both Salzkammergut sections (bedded grey limestones, literature data see Krystyn 1983, Orchard 1991, and Kozur 2003). Uppermost Langobardian (*regoledanus* ammonite zone) is evidenced by Gawlick et al. (1999a) in the lower part of the bedded grey limestones within the Jakobberg gallery. Uncertain is the presence of the *G. mostleri* conodont assemblage zone (abbreviated 'A. Z.') representing the lower *aonoides* ammonite zone or Julian 1/I (after Gallet et al. 1994) and of the *G. tadpole* Interval Zone (base of the upper *aonoides* ammonite zone or Julian $2/I_1$) in both sections. *G. mostleri* did not occur in the Freygutweg section and *G. tadpole* only very rarely (two specimens; Fig. 9f) in the middle part of the bedded grey limestones. The *Gl. tethydis* conodont assemblage zone (coexistence of *Gl. tethydis* Huckriede with *G. polygnathiformis*), representative for the upper *aonoides* ammonite zone and the *austriacum* ammonite zone (Julian 1/II to 2/II), includes the uppermost bedded grey limestones, the ochre-coloured limestones, and the Reingraben Shales. Because of the absence of *G. auriformis* and the abundance of *G. tethydis* (Figs. 9b–e, j) in the Salzkammergut sections we favor unlike to Krystyn (1983) the *Gl. tethydis* A. Z. As a result, the very depauperate fauna of *G. polygnathiformis* and *Gl. tethydis* allows only a general age assignment of Middle to Late Early Carnian (*aonoides* to *austriacum* ammonite zone resp. *tethydis* conodont zone). Stratigraphically important is the disappearance of *Gl. tethydis* on top of the shales. This proves the exclusive Lower Carnian age of the Reingraben terrigenous interval in the Hallstatt facies of Berchtesgaden and most probably elsewhere. Two lithological turnovers, a) the change of bedded grey limestones to ochre-coloured limestones and b), from ochre-coloured limestones to Reingraben Shales are embedded in this time interval. *Halobia rugosa* Gümbel, whose specimen were found by Medwenitsch (1949) in the Reingraben Shales of the Jakobberg gallery, has a first occurrence date at the beginning of the *austriacum* ammonite zone (Julian 2; see also Gruber (1976) and Krystyn in Gallet et al. (1994)). Following this, it is very likely to put the initial lithological change of the Reingraben Turnover exclusively within the uppermost *aonoides* ammonite zone and the *austriacum* ammonite zone (Julian 1/IIc to Julian 2).

The lithological boundary between Reingraben Shales and the nodular red flaser limestones is covalent to the beginning of the *G. polygnathiformis* A. Z. (Figs. 9k–o; *dilleri* ammonite zone and lower *subbullatus* ammonite zone, Tuvalian 1 to 2/I) and is conterminous to a third lithological event (change from Reingraben Shales to nodular red flaser limestones). The first occurrence date of *G. nodosa* (Fig. 9p) in bed 13 defines the *G. nodosa* A. Z. (upper *subbullatus* ammonite zone and upper *spinosus* ammonite zone or Tuvalian 2/II to 3/II) at the very base of the bedded light-coloured limestones. The uppermost Carnian conodont assemblage zone identified by *M. communisti* (uppermost *spinosus* zone) is evidenced by Gawlick et al. (1999a).

The last occurrence of *G. polygnathiformis* in bed 16 and the first occurrence of *G. navicula* Huckriede (Figs. 10a, c) one bed above defines the Carnian-Norian boundary. Together with *E. quadrata* (Figs. 10h–i), *E. spatulata* (Fig. 10f), *E. abneptis* (Figs. 10b, e), and *E. triangularis* (Fig. 10d), these conodont specimen indicate a condensed and mixed fauna of the basal Norian (Lacian 1 to Lacian 3). Therefore, the Carnian/Norian boundary in the Salzkammergut is not equivalent with the lithological change from nodular red flaser limestones to bedded light-coloured limestones.

Sedimentary facies

The description and interpretation of the lithofacies and microfacies are based on thin sections and faunal composition extracted from acid residues. Thin sections enabled microfacies analysis of the Carnian Turnover in the Hallstatt Red facies belt for the first time. Additionally, the faunal composition of every single bed gave further information about environmental conditions. The results are shown in Table 1 and Fig. 11.

Description of the main lithologies (nomenclature according to Mandl 1999)

1. *Bedded grey limestones:* Greyish-coloured filament-wackestones containing algal crusts similar to "*Tubiphytes*" as reefal elements, peloids, and intraclasts, mixed with pelagic components (radiolarians and planktic crinoids). Further faunal components are conodonts and fish teeth (Figs. 12a, 13a–b).
2. *Green marly limestones:* Greenish-coloured, pyrite bearing mud- to wackestones exclusively yielding filaments of type II (ostracod shales). Exposed only in the Jakobberg gallery (Figs. 13b–c).
3. *Dark grey limestones:* Dark grey-coloured pyrite flaser wackestones in the lower part and bioclastic mudstones in the upper part, respectively. Exposed only in the Jakobberg gallery (Fig. 13d).
4. *Ochre-coloured limestones:* Thinly alternating detritic flaser wackestones and thrombolite flaser bindstones. Characteristic are very thinly bedded interbeddings of thrombolite algal crusts and detrital, partly fixed clasts (calcite and quartz, see also Figs. 13e–f). In addition, the fauna is rather depleted, (common occurrence of filaments, rare foraminifers and crinoids, and very rare conodonts). "*Tubiphytes*"-like microbialites are absent. Exposed only in the Jakobberg gallery (Figs. 13e–h).
5. *Reingraben Shales:* They represent different lithologies ranging from unfossiliferous black shales in the lowermost part, intercalated burrowed biogenic wackestones in the lower and middle part, and unfossiliferous laminated mudstones as well as thin- to medium-bedded

Table 1 Facies interpretation spanning both sections. Shown are the main biogenic and abiogenic components as well as a brief interpretation. The units are classified after Dunham (1962). Abbreviation: SMF = "Standard Microfacies" and FZ = Facies Zone (after Flügel 2004)

Strat. Unit	Facies	(Micro)components	Interpretation	SMF Flügel 2004	FZ Flügel 2004
bedded light-coloured limestones (Freygutweg section) (Lacian)	**radiolarian mudstones and wackestones**	**filaments (type 2 = ostracod shells); radiolarians (micritized and calcified), "*Tubiphytes*"**	Limestones with allochthonous reefal detritus ("*Tubiphytes*", ostracods, gastropods) and autochthonous hemipelagic faunal elements (conodonts, filaments, radiolarians). Complete recovering of the system - moderate to high supply of carbonate due to normal producing adjacent carbonate platforms.	1-2	2-3
nodular red flaser limestones (Freygutweg Section) (Julian 2/2 - Tuvalian 3)	**upper part:** crinoid and radiolarian packstones	**planktic crinoids** (Fig. 12h, k), **radiolarians (calcified)** (Fig 12.c, j)	Strongly condensed by: **a)** a low rate of sedimentation (bioturbation, firmgrounds, see Fig. 12l-m), **b)** vertical and **c)** horizontal pressure solution => result: "pseudobreccia" (Fig. 12e, g). Moderate carbonate supply.	1-2	2-3
	middle part: filament and radiolarian packstones	**type 2 filaments, foraminifers, radiolarians (calcified), mud peloids**	Depletion of filaments towards the top, coevally increasing content of calcified radiolarians. "*Tubiphytes*"-like algal fragments are completely absent in the lower and middle part, the local appearence in the upper and upper most part signalised a gradual recovery of the adjacent carbonate factories.	3	3-4
	lower part: filament packstones	**filaments (type 1 = bivalve shells), type 2 filaments , planktic crinoids, radiolarians (calcified), mud peloids** (Fig. 12e-g).	**Red colour:** oxygen-rich bottom water, local Eh/pH potential within the sediment or near the sediment/water surface, absence of sulfate-reducing bacteria (Flügel 2004).	3	3-4
	basalmost part: extraclast packstones	**extraclasts, radiolarians (calcified)**	**Basal breccia** (thickness 4 cm) with reworked components from the uppermost calcareous Reingraben intercalations and filament-bearing clasts: hint of a sedimentary gap.	4	3-4
Reingraben Shales with calcareous intercalations (Freygutweg section & Jakobberg gallery) (Julian 2/I)	**upper part:** unfossiliferous marls **intercalated:** laminated mudstones	-	**Unfossiliferous laminated limy intercalations:** sudden increased moderate carbonate supply. Deposited basinwards by increased water circulation within a reducing setting (no epi- and endobenthos) (Fig. 12c).	RMF 5	3-4
	middle part: biogenic argillaceous marls biogenic wackestones	**type 2 filaments, planktic crinoids, radiolarians**	**Fossiliferous calcareous intercalations:** temporary recovery of the carbonate factory - moderate carbonate supply within the basins, improved living conditions (bioturbation - Figs. 12b, 13j) caused by increased water circulation. Change from anaerobic to dysaerobic and aerobic setting.	1-2	3-4
	lower part: pyrite-rich unfossiliferous black marls and clays	**foraminifers and type 2 filaments (very rare)**	**Reingraben Shales:** complete breakdown of the carbonate factory, much terrigenous input, stagnating to very little carbonate supply. Anaerobic, reduced setting. Absence of benthnic life. High content of organic matter (ca. 4.7 %).		
ochre-coloured limestones (Jakobberg gallery) (Julian 1/IIc - 2/I)	**ochre-coloured limestones:** detrital flaser wackestones thrombolite flaser bindstones	**thrombolites, crinoids, type 2 filaments, calciclasts, foraminifers**	**Ochre-coloured limestones:** Moderate carbonate supply in the lower part, towards the top decreased carbonate content - the partly present fine lamination is caused by alternating thrombolites and calciclastic layers (Fig. 13e-g). Synsedimentary movements can be retraced by sedimentary structures (Fig. 13h).	1-2 19	3-4
	dark grey limestones: biogenic mudstones pyrite flaser wackestones	**type 2 filaments, foraminifers, calciclasts**	**Dark grey limestones:** many calciclasts, eventually reworked from the massive variegated limestones below. Intensively dissolved by microstylolites enriched with clay and dispersed pyrite: mainly anaerobic setting under low to moderate carbonate supply. Towards the top improved living-conditions (bioturbation, no pyrite) (Fig. 13d).	1-2	3-4
	green marly limestones: filament mudstones	**type 2 filaments**	**Green marly lms.:** Stagnation of the rate of sedimentation abruptly caused the complete decline of the carbonate factories. Preferred orientation of filaments could be a feature of slight bottom currents without bioturbation and extensive vertical pressure solution (Fig. 13b-c).	3	3-4
bedded grey limestones (Freygutweg section & Jakobberg gallery) (?Langobardian - Julian 1/IIb)	**filament wackestones**	**type 2 filaments, "*Tubiphytes*", mud peloids, intraclasts, radiolarians (calcified)**	Limestones with allochthonous reefal detritus ("*Tubiphytes*") and autochthonous hemipelagic fauna (filaments, radiolarians). Similar to the bedded light-coloured limestones in the basal Norian (Fig. 13a, b). Moderate to high carbonate supply - firmground at the top signalising an abrupt decline of the depositional rate. The boundary to the green marly limestones is emphasised with thrombolite algal crusts and authigenic calcites (Fig. 13a).	1-2 5	2-3

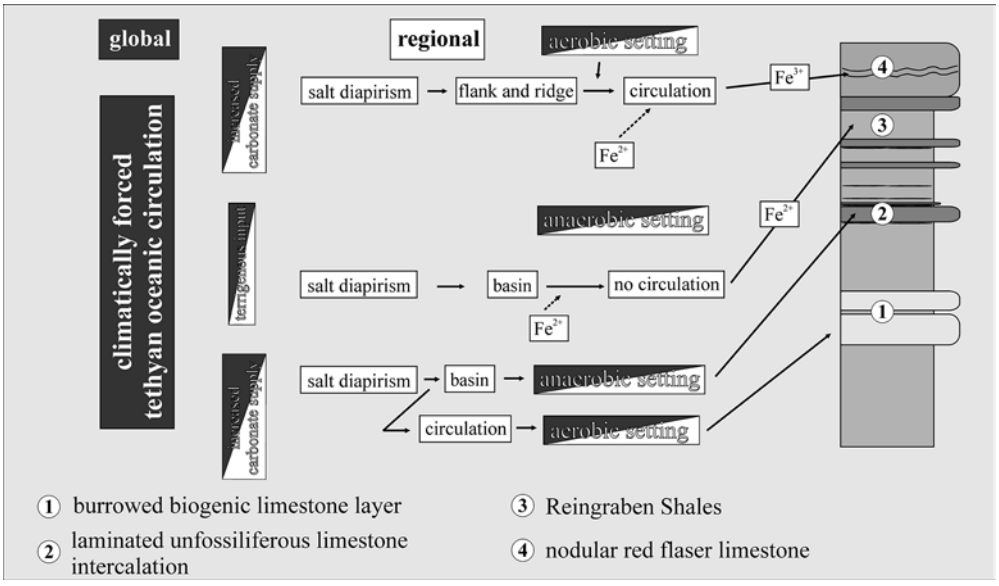

Fig. 11 Simplified facies model of the Hallstatt Basin with controlling global and regional factors, interpreted from the different lithologies within the Reingraben Shales and the nodular red flaser limestones

marls in the upper part (Figs. 12b–c, 13i–j). Faunal elements were found mostly in the burrowed calcareous intercalations. Notable is the occurrence of well-preserved *Osteocrinus* centrodorsalia within the middle part of the shales (Freygutweg section). Kristan-Tollmann (1970) recognized a global major appearance of osteocrinoids within the Ladinian to Carnian. All species, mentioned in this paper, were found in the Freygutweg section (Table 2).

6. *Nodular red flaser limestones:* Consisting of primary filament, radiolarian and crinoid packstones enriched with fine red biomicrites, this very condensed unit obtained its nodular texture ("pseudoclasts") through intensive horizontal and vertical pressure solution (Figs. 12e–m). The fauna consists mainly of filaments, radiolarians, crinoids, few gastropods, and rare complete ostracods. Whereas the frequency of filaments decreases towards the top, calcified radiolarians and crinoids increase. In the lower and middle parts, *Tubiphytes*-like algal crusts are completely absent. In the topmost part, they are sporadically present.
7. *Bedded light-coloured limestones:* The mud- and wackestones are rich in calcified radiolarians. Fewer faunal components are gastropods, juvenile ammonites, and filaments. The reoccurrence of *Tubiphytes*-like organisms indicate some reefal influence again.

Interpretation (see also Table 1)

The stratigraphic succession, represented by the sections, can be assigned to the flanks of synsedimentary ridges. This emanated from the stratigraphic model after Mandl (1984, 1999; see also Fig. 3) with regard to the varying palaeotopography. Whereas the basins expose marl dominating sequences, the top of the ridges show an ongoing calcareous sedimentation. These two main lithologies interfingered towards the flanks.

The bedded grey limestones represent ancient periplatform-mud with reefal influence, deposited within a deeper, low-energy setting under normal environmental conditions. This is evidenced by epifaunal elements like gastropods and an intact endofauna (intensely burrowing and churning). Microbial algal crusts near the top of the bedded grey limestones point to an incipient change in environmental settings, turning to a minor supply of oxygen. The crusts enclose fine, probably authigenic calciclasts, which were generated due to a reducing micromilieu (Fig. 13b; see Reitner 1997). The very top of the bedded grey limestones exhibits an undulating and intensely burrowed surface, which can be interpreted as firmground and, therefore, represents a sedimentary gap (Fig. 13b). Densely packed, oriented filaments (Figs. 13b–c) within the overlying thin-bedded green marly limestones indicate very low accumulation rates under low-energy setting. No signs of bioturbation do affirm this observation. The complete absence of endofaunal elements proceed in the lower part of the dark grey limestones, whereas their upper part shows intensive burrowing again.

The main part of the ochre-coloured limestones consists of densely laminated bindstones which were deposited within dysaerobic settings ("biofilms"; see also Wilderer and Charaklis (1989), Reitner et al. (1995), and Reitner (1997)) in starved basins (Figs. 13e–g). The minor part consisting of bioclastic and lithoclastic packstone intercalations with synsedimentary structures retraces the above-mentioned diapiric movements (Fig. 13h).

The Reingraben Shales in both successions represent a restricted, almost anoxic setting under high terrigenous influx and very low carbonate supply. The distinct boundary occurring between ochre-coloured limestones and black Reingraben Shales (Figs. 5c, 13i) most likely was under-

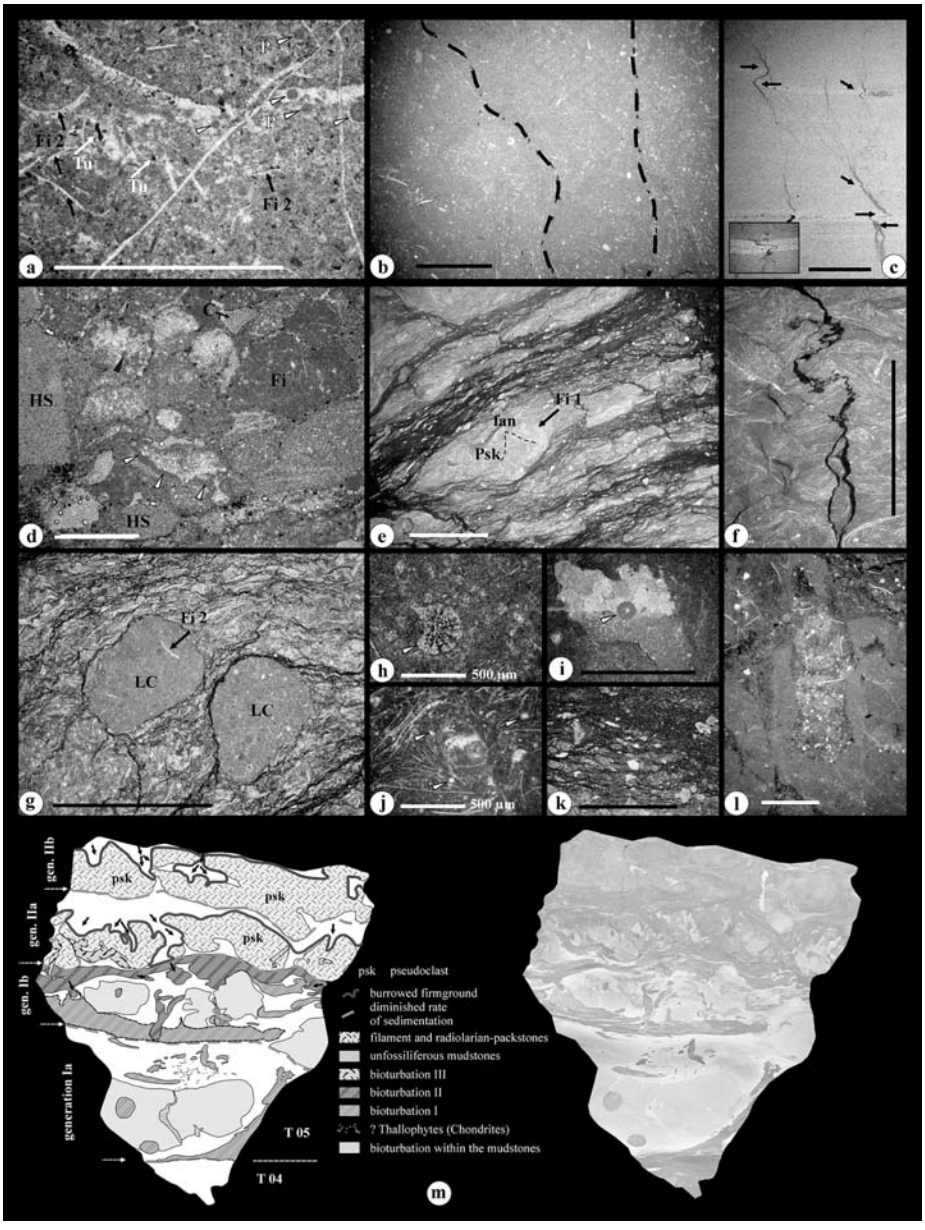

Fig. 12 Thin sections of the Freygutweg succession: **a** Bedded grey limestones: similar to the Jakobberg gallery (Fig. 13a) containing a high percentage of allochthonous, reef-derived organisms: tiny, arcuate filaments of type 2 (*black arrows*), fragments of "*Tubiphytes*"-like algal relics (*white arrows*) and mud peloids (*white triangles*). All bioclasts occur without preferred orientation. **b** Biogenic "Reingraben" limestones: single calcareous intercalation, rich in filaments (mostly type 2), radiolarians, planktic crinoids, and foraminifers. The wackestone is intensely burrowed, large bioturbation tracks (e.g., worm or holothuroid-burrows) mostly show a blurred borderline to the surrounding matrix (accentuated with a dashed line). **c** Reingraben Shales/thinly laminated silty carbonate: nearly undisturbed lamination characterised by alternating limestone and clay-rich layers, pervaded and dissolved by horizontal stylolites. The direction of these stylolites changed in the more competent limestone layers (*thin black arrows*). **d** Lowermost nodular red flaser limestones: transition zone between the uppermost calcareous "Reingraben" interbeds and the nodular red flaser limestones. This zone (thickness circa 4 cm) is characterised by a breccia containing different, mostly angular components: disarticulated crinoid fragments (C), filament-bearing limestone intraclasts (Fi) and extraclasts similar to those occurring in bedded silty carbonate embedments (HS) underneath. Also notable are micritic envelopes (cortoids) formed by microborers (black triangles) in combination with micrite precipitation (*white triangles*). The angular lithoclasts are etched and rounded due to pressure solution. **e** Nodular red flaser limestones: the whole unit is characterised by etched "pseudoclasts" (Psk), formed by extensive pressure solution. These "pseudoclasts" bear filaments indicating a low rate of sedimentation and burrowing, the lack of orientation is caused by intensive bioturbation ("fan"). **f** Angled suture line of a horizontal stylolite enriched with reddish clay (nodular red flaser limestones). **g** Lithoclasts (LC) within a filament-bearing, altered intensively by micro-pressure solution. **h** Dorsal floating wing of a planktic crinoid (*Osteocrinus* sp.). **i** Geopetal texture showing a loosely packed peloidal internal filling, overgrown by spar. The round structure is a crinoid-fragment (*white triangle*). **j** Calcified radiolarians were most abundant in the upper parts of nodular red flaser limestones (white triangles). **k** The boundary between "pseudoclasts" and the surrounding biomicritices is often enriched with fragments of planktic crinoids (here; brachialia). **l** Burrows in a firmground filled with sediment rich in radiolarians and some filaments. **m** Example of several distinct hardgrounds representing phases of a reduced sedimentation within a single horizon (in this case: T 05, thickness circa 12 cm). Note: Scale bar all 1 mm

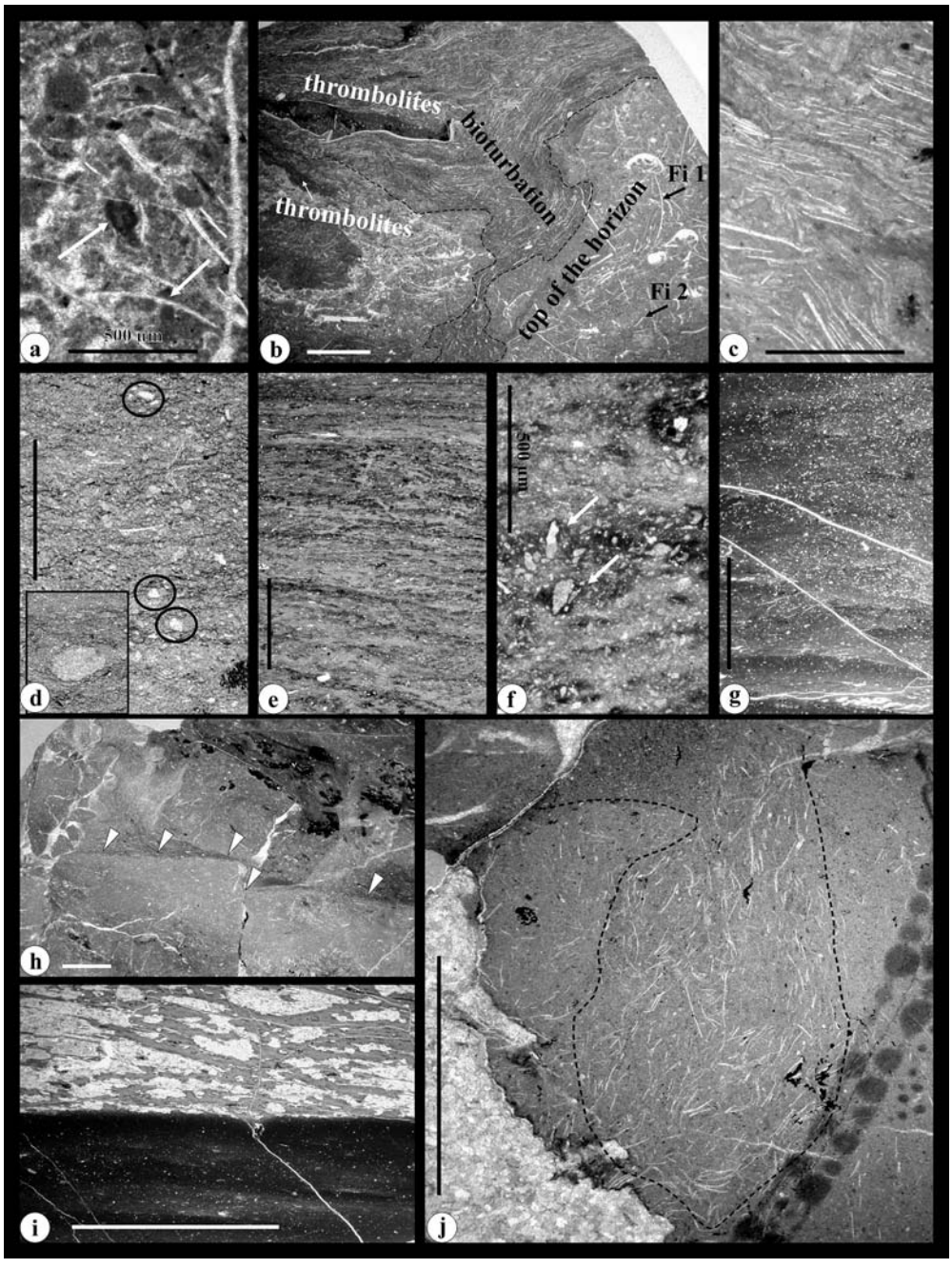

Fig. 13 Thin sections from the Jakobberg gallery section: **a** The top of bedded grey limestones contains a high percentage of allochthonous reef-derived organisms: of major importance are "*Tubiphytes*"-like fragments (*thin white arrow*). **b** The very top of the bedded grey limestones is characterised by strongly reduced rate of sedimentation, strong bioturbation, firmgrounds, thrombolite crusts with authigene calcite particles and the coeval diminished occurrence of *"Tubiphytes"*-like fragments. Fi 1 = type 1 filament, Fi 2 = type 2 filament. **c** The green marly limestones show preferred orientation of densely packed filaments (type 2) defining the lower boundary of the Reingraben Turnover in the Hallstatt basin (Salzberg facies area). **d** Bedded dark grey limestones (pyrite-rich phacoidal wackestones): detrital calcites are very common and might be equated to reworked authigene calcites from the layers underneath. **e–h** Ochre-coloured limestones (thrombolite bindstones): The horizons are characterised by micro-alternations between detrital calcites and cloudy microbialite. The latter have encrusted and stabilised the calciclasts deposited beforehand. There are also synsedimentary shifts, sealed with crinoid- and calciclast-rich wackestones. **i** The boundary between the ochre-coloured limestones and black Reingraben Shales is very distinctive (also in thin sections) coinciding with a sudden increase of organic matter. **j** The basal "Reingraben" limestone intercalation has been intensively churned by bioturbation. The filaments (type 2) contoured the burrows (accentuated with dashed line). Note: Scale bar all 1 mm

Table 2 Faunal composition of the Freygutweg section and the Jakobberg gallery. White circles: rare; grey circles: common; full black circles: abundant

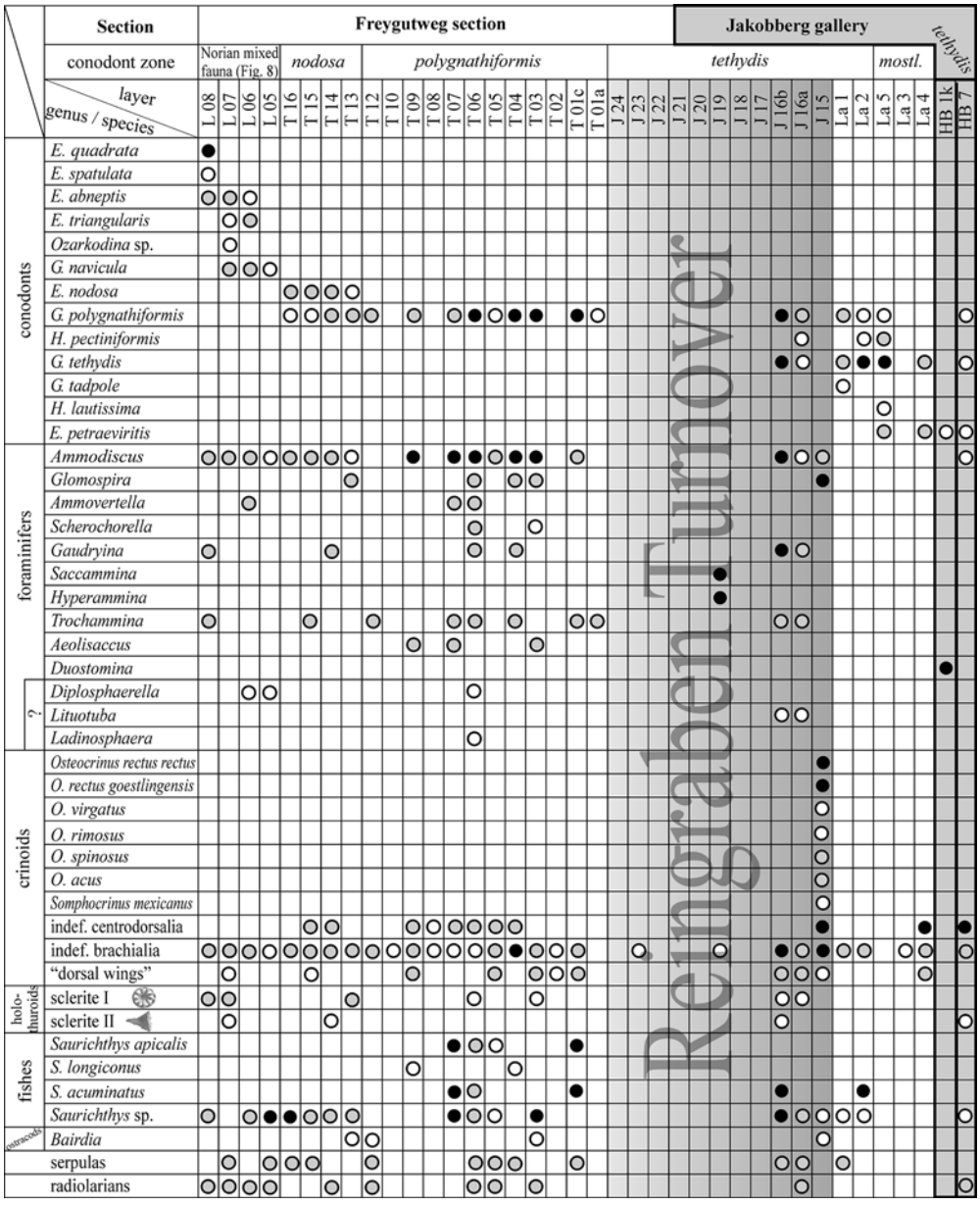

lined by diagenetic conditions: most of the goethite contained within the ochre-coloured limestones is certainly not primary but was oxidised from pyrite due to oxygen-enriched pore water drainage. At the almost impermeable black shales, pore-water circulation stopped and so did oxidation of pyrite. Therefore, this lithological change in the Jakobberg gallery is interpreted as a combination of primary induced change in the depositional and ecological setting with subsequent diagenetic overprint. The anoxic Reingraben Shales are completely unfossiliferous and yield neither neritic nor planktic or epibenthic forms. The complete lack of bioturbation implies the absence of endobenthic life. The ancient microlamination, which probably existed beforehand, has now been overprinted by micro pressure solution.

The intercalated limestones in between the Reingraben Shales are interpreted as "event beds", deposited during short recreation phases of the carbonate factory. We differ between bioclastic, burrowed, and "homogenised" interbeddings with allochthonous planktic components in the lower and middle parts (Figs. 12b, 13j) and thinly laminated, unfossiliferous intercalations in the upper part (Fig. 12c). Most likely, the intercalated limestones represent an acyclic succession of downslope calcareous suspension flows, which swept into the basins triggered by, e.g., regional storm events. In combination with a basin-spanning circulation period and, thus, oxygen-enrichment in the once starved basins, epi- and endobenthic life increased during short time intervals— the beds were burrowed intensely. The unfossiliferous interbeds were related

to anoxic conditions. The absence of benthic life led to a preservation of the primary microlamination.

The frequency of unfossiliferous calcareous intercalations increases within the upper part of the Reingraben Shales before deposition of the nodular red flaser limestones. Thus, the depositional regime graded from clay to limestone-dominated sediments, first of all under anoxic conditions, then under aerobic bottom water.

The distinctive boundary between Reingraben Shales and nodular red flaser limestones can be explained by a drastic change in water circulation patterns. The boundary between the topmost laminated calcareous "Reingraben" interbedding and the basalmost red nodular flaser limestone bed exhibits a short stratigraphical gap represented by a thin-bedded breccia (thickness about 4 cm; see Fig. 12d). The well medium-bedded red limestones graduated to bedded light-coloured limestones which contain reefal components such as *Tubiphytes*, crinoids, and peloids again. This should not be interpreted as a basinward progradation of the adjacent shelves rather than a slightly recovered carbonate system and, therefore, an increased carbonate supply.

This overview of the lithology describes at least three abrupt and drastic changes in lithology and mineralogy, which were presumably due to the following superimposed controlling global as well as regional factors (in order of importance): **(a)** global, probably tethyan-wide variations in oceanic circulation and oxygen supply, **(b)** the varying regional topography of the oceanographic palaeo-relief and **(c)** differences in the ratio between carbonate supply and terrigenous influx. These are now discussed:

(a) Due to the presence of pyrite in the Reingraben Shales, we can assume an Eh/pH-potential near the sediment–water interface. As a result, the increased iron input deriving from the weathering of terrigenous material, was reduced to pyrite. The red colour of the limestones, however, indicates oxidation of iron into hematite. According to this interpretation, the seafloor relief had evidently led to different levels of circulation: 1) low circulation and a reducing, anaerobic setting in the flat basins of the Hallstatt Grey facies and 2) moderate circulation and dysaerobic bottom water upon the top and flanks of the ridges within the Hallstatt Red facies. Due to the mobility of the submarine relief with time, the boundary between anaerobic and aerobic bottom water changed upon the flanks (red limestones). Only the deeper regions of the flat basins are assumed to have remained constantly anaerobic.

(b) The topography was controlled by the mobile Permian Haselgebirge and had the form of elongated ridges and intervening shallow basins. Nodular red flaser limestones were deposited upon the ridges and their flanks, interfingering with black Reingraben Shales at the bottom of the flanks (Situation in the Julian 2; see Fig. 3).

(c) The above-mentioned "event beds" within the Reingraben Shales affirm the thesis of Reijmer and Everaas (1991): they showed from a Rhaetian example in the Southern Alps, that the Carnian basins were profoundly conditioned by the development of the adjacent shelves. At times of short recreations, increased mud supply caused calcareous suspension flows into the basins intermitting the monotonous series of black shales (Fig. 14).

Water depth

The close relationship between shelf and adjacent basin requires diminished basinal water depth. Bathymetric reconstructions have been discussed controversially in the last decades (a compilation of several authors was published by Rieche (1971) as well as Wendt and Aigner (1985)). Later investigations (Reading 1986 and Schmidt 1990) favoured water depths of 70–100 m.

Isotopes

Oxygen and carbon ratios were measured in all calcareous and marly beds to interpret primary ecologic and secondary diagenetic overprints.

Due to the complete lack of brachiopods and belemnites for analysis, four whole-rock samples were extracted instead from every bed (weights between 0.05 and 0.37 mg) with a dental drill. Attention was paid to obtain mudstones without late cements derived from shell cavities and fissure fills. The average of the values (best three of four) represents the isotope ratio which is pictured in Figs. 7 and 8. Isotopic analyses were performed with a Thermo Quest Finnigan Delta Plus XL spectrometer. The results are expressed in δ‰units and reported against the V-PDB standard. The reproducibility for the isotope determinations was $\pm$ 0.2 ‰(1σ) for $\delta^{18}O$ and $\pm$ 0.1 ‰(1σ) for $\delta^{13}C$.

As for the $\delta^{13}C$ values, the combined succession of both the Freygutweg section and the Jakobberg gallery show a slightly increasing trend within the bedded grey limestones (2.7–3.2 ‰), decreases slightly in the ochre-coloured limestones (2.0–3.0 ‰) and increases again towards the nodular red flaser limestones and bedded light-coloured limestones (max. 3.8 ‰). In contrast, the $\delta^{18}O$ values decrease: Very "heavy" values prevail, ranging from 0.4 to -0.8 in the uppermost part of bedded grey limestones to about -1 to -1.5 ("lighter values") in the nodular red flaser limestones and the bedded light-coloured limestones.

Marshall (1981) published very similar $\delta^{18}O$ values from Jurassic and Triassic Tethyan limestones of several sections in Sicily and northern Italy. He points out that the "heavy" $\delta^{18}O$ values in pelagic chalks and limestone nodules originated from early high-magnesium calcite cements rather than from an abnormal sea-water composition. Also, Bellanca et al. (1995) described similar "heavy" $\delta^{18}O$ values from Carnian deep-water limestone and marls from the Sicani Mountains, Sicily. In their paper, Julian dark marls with interbedded calcilutites show almost negative $\delta^{13}C$ values. These marls were assumed to have been deposited in a basin with "dominantly anoxic to dysaerobic bottom waters". In contrast, the ochre-coloured limestones

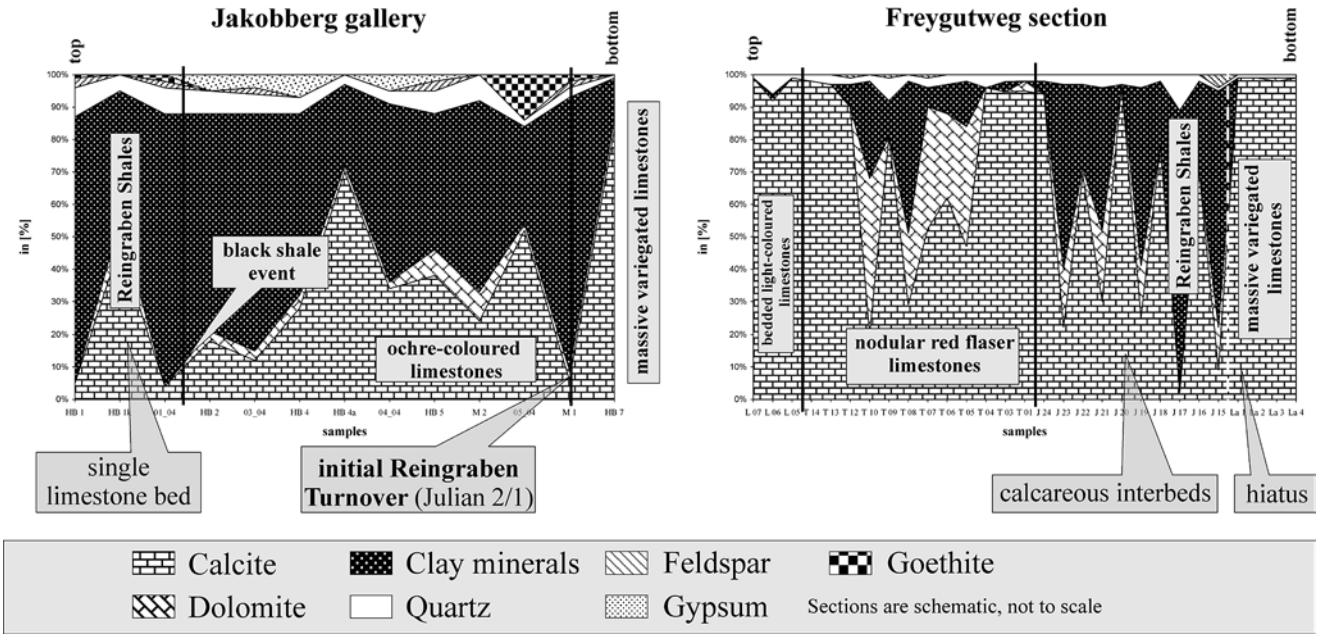

Fig. 14 Rock composition of the two sections, based on X-Ray fluorescence analysis

and black Reingraben Shales, described in this paper, which were also considered to be deposited within a locally restricted basin, show positive $\delta^{13}C$ values and do not confirm this. As there is no signal in $\delta^{13}C$ through the transition from the bedded grey limestones to the Reingraben Shales, it is assumed that there was no marked or substantial change in seawater chemistry during the Reingraben Turnover. Keim and Brandner (unpublished data) have gained similar results from starved basins in the Southern Alps.

X-ray data

In addition to biochronology and facies interpretation, all beds underwent X-ray fluorescence analysis to identify the main mineral composition. The samples were pulverised and measured by a Siemens D-500 X-Ray Diffractometer (standard operating procedure). The simplified "translation" into graphic data, as shown in Fig. 11, was computed using "Analysis Technique for Rock Material, RVS 11.062, edition 1987". This is a semiquantitative method to calculate the main components of rock material such as calcium carbonate, dolomite, clay minerals, quartz, feldspar, micas, gypsum, and goethite. The absolute percentage matter of accessorial dispersed pyrite, observed in thin sections of the dark grey limestones and calcareous "Reingraben" interbeds, respectively, was below the detection limit.

Some remarks must be given regarding gypsum, goethite, and dolomite. After deposition, gypsum recrystallised in the gallery as a secondary precipitation of salt and is enriched in fine molds and minor joints. Goethite was oxidised by oxygen-rich drainage water. Dolomite sprouted as crystals near stylolites and minor joints.

Figure 11 illustrates a sudden increase of terrigenous influx (mainly clay minerals) occurring with deposition of the Reingraben Shales. The short-term interferences in the content of calcium carbonate within the ochre-coloured limestones and Reingraben Shales have been caused by calcareous interbeds. The basal part of the nodular red flaser limestones reveal high carbonate contents, which decrease towards the top of this unit. The top of the red limestones and the bedded light-coloured limestones show a similar composition: as discussed in the section on biostratigraphy, the lithological boundary is not identical with the biostratigraphic boundary.

Discussion

The Reingraben Turnover is only one regional synonyme for a synchronous series of similar major sedimentary changes, traceable throughout the whole Tethyan realm (e.g., Martini et al. 2000; L. Krystyn pers. comm., Vienna) at the beginning of the Late Triassic. Despite having different names, all turnovers are comparable by their sudden influx of large amounts of siliciclastics and anoxic sediments, combined with local extinction events and a depleted fauna (e.g., Simms and Ruffel 1989; Krystyn 1991). The siliciclastic material covered the carbonate platforms and shelves unconformly and, according to most theories, should have caused an abrupt decline of almost all Tethyan carbonate factories. It is still disputed, and there is need of further investigations, whether the reefs were (a) aerially exposed, (b) had been drowned due to an increased subsidence rate, or (c) had been degenerated by a forced siliciclastic input combined with anoxia. These points are now discussed in detail:

(a) There is evidence of aerial exposure due to the existence of palaeokarst features in shallow-water facies, probably caused by a dramatic regression (e.g.,

Bechstädt and Dohler-Hirner 1983; Mutti and Weissert 1995).

(b) Continuous stratigraphic successions existing in the Wetterstein facies belt (e.g., Angermeier et al. 1963). Brandner (1984) explained the regional differences in lithology, namely continuous and discontinuous successions between Wetterstein Limestone and Raibl Beds and their equivalents, with regional tilting of tectonic blocks. However, exact evidence for reef drowning in the Carnian is still missing.

(c) According to Hallock and Schlager (1986), extensional tectonic processes are too slow to drown a carbonate platform. They offer another explanation. The decline of the carbonate factory is generated by nutrient excess. In the Carnian period, this nutrient overflow might have been caused by increased terrigenous input. This resulted in increased bioproductivity, major water pulp, and, at least, minor productivity of the carbonate factory.

As shown in the section on biochronostratigraphy, the Hallstatt sequence should mirror the platform and shelf development temporally delayed in the basin: the terrigenous input covering the platforms (wherever exposed or drowned) caused a decline in the carbonate production during a regressional stage (e.g., Brandner 1984; Hallock and Schlager 1986; Mandl 1999). This is indicated by the diminished depositional rate on top of the bedded grey limestones (Fig. 13b). Subsequently, the siliciclastic material, mainly clay mixed with quartz, feldspar, micas, etc., was swept into the basins. Whereas intraplatform basins (Reifling Basin) were filled completely with clay and sand (Lunz Sandstones) with a thickness of more than 200 m, terrigenous deposits in the Hallstatt Basin amount only a few metres. In the Hallstatt Basin, the first terrigenous sign produced a distinct boundary indicated by the first appearance of green marly limestones (Jakobberg gallery). The subsequent clay-dominated sedimentation (Reingraben Shales) is evidence of a reducing, starved basin without water circulation. The fact that the occurrences of black shales are not persistently traceable may have—apart from secondary tectonical shearing—also sedimentary reasons: As discussed before, the submarine topography was characterised by synsedimentary ridges and several interjacent flat basins. These starved basins probably were connected to each other, but eventually became isolated causing coeval depositions of black shales, whereas on top of the ridges carbonate sedimentation was interrupted by condensed horizons. From the stable isotopic data we can assume that the general chemistry of ocean water perhaps was fairly uniform during the whole Carnian—a "global black shale event" ought to be marked by sharp and distinct shifts in $\delta^{13}C$ values.

In the Upper Julian, an incipient transgression, combined with a slow recovery of the platforms led to the formation of condensed limestones with less clay and quartz (nodular red flaser limestones). The bedded light-coloured limestones indicate a return to "normal" sedimentary conditions: the shelves recovered completely during a transgressional pulse in the basal Norian (Mandl 1999).

Finally, two superimposed factors could have caused the sudden increase of terrigenous influx: (a) changed plate constellations and orogenic events, and (b) a, therefore, forced continental (monsoonal) climate, discussed as followed:

(a) As is noted in the section on palaeogeography, the event happened in a time of general plate rearrangement. Within the NCA, the terrigenous event might be relatable to the Kimmerian orogeny of the eastern northern Tethys (Brandner 1984; Bechstädt and Schweizer 1991) as well as the flexural uplifting of the Fennoscandian High (Aigner and Bachmann 1992). The latter might have caused a decreased rate of subsidence and a flat shelf (prograding carbonate platforms, e.g., Brandner 1984; Bechstädt and Schweizer 1991; Mandl 1999) and large amounts of weathering products.

(b) Due to the very large landmass of Pangea, climate conditions must have been very similar to those of present Asia. Therefore, Hay et al. (1994) and Mutti and Weissert (1995) postulated "megamonsoonal" climates for Pangea and the Tethyan realm. During the Middle and Late Carnian, increased rainfall and humid weathering conditions generated large amounts of fluvial sediments (Simms and Ruffel 1989). The "Schilfsandstein" and comparable deposits unconformly covered the Mid European realm by a thickness of 20 m (Aigner and Bachmann 1992) and were transported south-eastwards towards the Tethys. This fact is evidenced not only by the widespread siliciclastic coverings in Europe, but also by extinction events (Simms and Ruffel 1989).

Conclusions

The Reingraben Turnover was studied at two sections near Bad Dürrnberg, Austria, using a multistratigraphical approach. Based on biochronostratigraphy, the lithological change could be placed in the uppermost *aonoides* ammonite zone and the *austriacum* ammonite zone (Julian 1/IIc–2/II). This lithological change should not be understood as a rapid "event", implying a very short time gap. The Turnover can rather be split into three "events" which reflected, temporally delayed with regards to the carbonate platform and shelf evolution, the basinal development: a) Increased terrigenous input weakened the carbonate factory on the shelves and led to stagnating basinal deposition rates, followed b) by the initiation of black shales. The abrupt turnover to sedimentation under aerobic setting is marked by the c) red nodular flaser limestones. Finally, d) the slow recovering of the adjacent shelf is reflected in carbonate sedimentation towards the basins.

Microfacies analysis affirmed the high dependency of the Hallstatt Basin on adjacent carbonate factories, combined

with varying water circulation, oxygen supply, and local tectonics, such as syndepositional movements.

Stable isotopic datasets show no significant change in water chemistry during the whole Carnian emphasising that the black shale event was without global relevance.

Climate changes, for example, increased precipitation caused by megamonsoonal activity related to changes in plate assemblage, are presumed to have been the superimposed, global factors that trigger very similar, maybe comparable events throughout the Tethyan realm.

Acknowledgements We thank Helmut Lindtner, Bad Dürrnberg, for permission to sample the Freygutweg section on his private property, Hans-Jürgen Gawlick (University of Leoben) for help during the initial field trip, Werner Prochenberger for authorisation to enter the Jakobberg gallery, and Foreman Thomas Grublacher (both Bad Dürrnberg) for assistance during sampling. We are sincerely grateful to Leopold Krystyn (Vienna) for useful hints with regard to biostratigraphy and conodont speciation, Antonio Donofrio for classifying the conodonts, Werner Resch for microfaunal speciation, Richard Tessadri for X-Ray analyses, Christoph Spötl for stable isotopic measurements and discussing the data, Diethard Sanders for inspiring discussions and hints with regard to the manuscript, and last but not least Bernard Millen (all Innsbruck) for reviewing the manuscript. Furthermore we thank the FWF (Fund No. P16878) for financial support.

References

Aigner T, Bachmann GH (1992) Sequence stratigraphic framework of the German Triassic. Sediment Geol 80:115–135

Angermeier HO, Pöschl A, Schneider HJ (1963) Die Gliederung der Raibler Schichten und die Ausbildung ihrer Liegendgrenze in der „Tirolischen Einheit" der östlichen Chiemgauer Alpen. Mitt Bayer Staatssamml Paläont Hist Geol 3:83–105

Bechstädt T, Dohler-Hirner B (1983) Lead-zinc deposits of Bleiberg-Kreuth. In: Scholle PA, Bebout DG, Moore CH (eds) Carbonate Depositional Environments. Amer Assoc Petrol Geol Mem 33:55–63

Bechstädt T, Schweizer T (1991) The carbonate-clastic cycles of the East-Alpine Raibl group: result of third-order sea-level fluctuations in the Carnian. Sediment Geol 70:241–270

Bellanca A, Di Stefano P, Neri R (1995) Sedimentology and isotope geochemistry of Carnian deep-water marl/limestone deposits from the Sicani Mountains, Sicily: Environmental implications and evidence for planktonic source of lime mud. Palaeogeogr Palaeoclimatol Palaeoecol 114:111–129

Brandner R (1984) Meeresspiegelschwankungen und Tektonik in der Trias der NW-Tethys. Jb Geol Bundesanst 126:435–475

Braun R (1998) Die Geologie des Hohen Gölls. Forschungsberichte Nationalpark, Berchtesgaden, 192 pp

Decker K, Faupl P, Müller A (1987) Synorogenic sedimentation on the Northern Calcareous Alps during the Early Cretaceous. In: Flügel HW, Faupl P (eds) Geodynamics of the Eastern Alps. Deutike, pp 126–141

Dunham RJ (1962) Classification of carbonate rocks according to depositional texture. Amer Assoc Petrol Mem 1:108–121

Flügel E (2004) Microfacies of carbonate rocks—Analysis, Interpretation and Application. Springer, Berlin Heidelberg New York

Flügel E, Senowbari-Daryan B (2000) Triassic reefs of the Tethys. In: Stanley GD (ed) The History and Sedimentology of Ancient Reef Systems. Topics in Geobiology. Plenum, New York, pp 217–249

Frank W (1987) Evolution of the Austroalpine Elements in the Cretaceous. In: Flügel HW, Faupl P (eds) Geodynamics of the Eastern Alps. Deutike, pp 379–406

Frisch W, Gawlick HJ (2003) The nappe structure of the central Northern Calcareous Alps and its disintegration during Miocene tectonic extrusion —a contribution to understanding the orogenic evolution of the Eastern Alps. Int J Earth Sci 92:712–727

Gallet Y, Besse J, Krystyn L, Théveniaut H, Marcoux J (1994) Magnetostratigraphy of the Mayerling section (Austria) and Erenkolu Mezarlik (Turkey) section: improvement of the Carnian (late Triassic) magnetic polarity time scale. Earth Planet Sci Lett 125:173–191

Gawlick HJ (2000) Paläogeographie der Obertrias-Karbonatplattformen in den Nördlichen Kalkalpen. Mitt Ges Geol Bergbaustud Österr 44:46–95

Gawlick HJ, Diersche V (2000) Die Radiolaritbecken in den Nördlichen Kalkalpen (hoher Mittel-Jura, Ober-Jura). Mitt Ges Geol Bergbaustud Österr 44:97–156

Gawlick HJ, Lein R (1997) Neue stratigraphische und fazielle Daten aus dem Jakobberg- und Wolfdietrichstollen des Hallein-Bad Dürrnberger Salzberges und ihre Bedeutung für die Interpretation der geologischen Verhältnisse im Bereich der Hallein—Berchtesgadener Schollenregion. Geol Paläont Mitt Innsbruck 22:199–225

Gawlick HJ, Lein R (2000) Die Salzlagerstätte Hallein—Bad Dürrnberg. Mitt Ges Geol Bergbaustud Österr 44:263–280

Gawlick HJ, Lein R, Piros O, Pytel C (1999a) Zur Stratigraphie und Tektonik des Hallein—Bad Dürrnberger Salzberges—Neuergebnisse auf der Basis von stratigraphischen und faziellen Daten (Nördliche Kalkalpen, Salzburg). Abh Geol Bundesanst 56:69–90

Gawlick HJ, Frisch W, Vescei T, Steiger F, Böhm F (1999b) The change from rifting to thrusting in the Northern Calcareous Alps as recorded in Jurassic sediments. Geol Rundsch 87:644–657

Grottenthaler W (1978) Die Raibler Schichten der Nördlichen Kalkalpen zwischen Salzach und Phyrnpaß—Lithofazielle, sedimentologische und paläogeographische Untersuchungen. Mitt Ges Geol Bergbaustud Österr 25:11–33

Gruber B (1976) Neue Ergebnisse auf dem Gebiete der Ökologie, Stratigraphie und Phylogenie der Halobien (Bivalvia). Mitt Geol Ges Bergbaustud Österr 23:181–193

Hallock P, Schlager W (1986) Nutrient excess and the demise of coral reefs and carbonate platforms. Palaios 1:389–398

Hay WW, Thompson S, Pollard D, Wilson KM, Wolc C (1994) Results of a climatic model for Triassic Pangea. Z Geol Paläont Teil 1 H 11/12:1253–1265

Jerz H (1966) Untersuchungen über Stoffbestand, Bildungsbedingungen und Paläogeographie der Raibler Schichten zwischen Lech und Inn (Nördliche Kalkalpen). Geol Bavar 56:1–99

Keim L, Brandner R, Krystyn L, Mette W (2001) Termination of carbonate slope progradation: an example from the Carnian of the Dolomites, Northern Italy. Sediment Geol 143:303–323

Kozur H (2003) Integrated ammonoid, conodont and radiolarian zonation of the Triassic and some remarks to Stage/Substage subdivision and the numeric age of the Triassic stages. Albertiana 28:57–74

Kristan-Tollmann E (1970) Die Osteocrinusfazies, ein Leithorizont von Schwebcrinoiden im Oberladin—Unterkarn der Tethys. Erdöl und Kohle 23:781–789

Krystyn L (1970) Zur Conodonten-Stratigraphie in den Hallstätter Kalken des Salzkammergutes (Österreich). Verh Geol Bundesanst 1970:497–502

Krystyn L (1973) Zur Ammoniten- und Conodonten-Stratigraphie der Hallstätter Obertrias (Salzkammergut, Österreich). Verh Geol Bundesanst 1973:112–153

Krystyn L (1978) Eine neue Zonengliederung im alpin-mediterranen Unterkarn. Schriftenr Erdwiss Komm Österr Akad Wiss 4:37–75

Krystyn L (1980) Triassic conodont localities of the Salzkammergut Region (Northern Calcareous Alps). In: Schönlaub HP (ed) Second European Conodont Symposium, Guidebook and Abstracts. Abh Geol Bundesanst, pp 61–99

Krystyn L (1983) The Epidauros Section (Greece)—a contribution to the conodont standard zonation of the Ladinian and Lower Carnian of the Tethys Realm (Englisch translation). Schriftenr Erdwiss Komm 5:231–258
Krystyn L (1991) Die Fossillagerstätten der alpinen Trias. Exkursionsführer, pp 23–78
Krystyn L, Gallet Y, Besse J, Marcoux J (2002) Integrated Upper Carnian to Lower Norian biochronology and implications for the Upper Triassic magnetic polarity time scale. Earth Planet Sci Lett 203:343–351
Mandl GW (1984) Zur Trias des Hallstätter Raumes—ein Modell am Beispiel Salzkammergut (NKA, Österreich). Mitt Ges Geol Bergbaustud Österr 30/31:133–176
Mandl GW (1999) The Alpine sector of the Tethyan Shelf—Examples of Triassic to Jurassic sedimentation and deformation from the Northern Calcareous Alps. Mitt Österr Geol Ges 92:61–79
Mandl GW, Ondrejickova A (1993) Radiolarien und Conodonten aus dem Meliatikum im Ostabschnitt der Nördlichen Kalkalpen (Österreich). Jb Geol Bundesanst 136:841–876
Marshall JD (1981) Stable isotope evidence for the environment of lithification of some Tethyan limestones. N Jb Geol Paläont Mh 4:211–224
Martini R, Zaninetti L, Villeneuve M, Corne JJ, Krystyn L, Cirilli S, De Wever P, Dumitrica P, Harsolumakso A (2000) Triassic pelagic deposits of Timor: palaeogeographic and sea-level implications. Palaeogeogr Palaeoclimatol Palaeoecol 160:123–151
Medwenitsch W (1949) Fossilfund im Halleiner Salzberg. Berg-Hüttenmänn Mh 94:65–66
Medwenitsch W (1958) Zur Geologie des Halleiner Salzberges. Die Profile des Jakobberg- und Wolfdietrichstollens. Mitt Geol Ges Wien 51:197–218
Medwenitsch W (1962) Die Bedeutung der Grubenaufschlüsse des Halleiner Salzberges für die Geologie des Ostrandes der Berchtesgadener Schubmasse. Z Dt Geol Ges 113:463–494
Medwenitsch W (1963) Zur Geologie des Halleiner und Berchtesgadener Salzberges. Mitt Naturwiss Arbeitsgem Haus Natur 1963:1–18
Mutti M, Weissert H (1995) Triassic monsoonal climate and its signature in Ladinian-Carnian carbonate platforms (Southern Alps, Italy). J Sediment Res 65b:357–367
Neubauer F (1994) Kontinentkollision in den Ostalpen. Geowissenschaften 12:136–140
O'Neil JR, Clayton RN, Meyeda TK (1969) Oxygen isotope fractionation in divalent metal carbonate. J Chem Phys 51:5547–5558
Orchard, MJ (1991) Upper Triassic conodont biochronology and new index species from the Canadian Cordillera. In: Orchard MJ, McCracken AD (eds) Ordovician to Triassic Conodont Paleontology of the Canadian Cordillera. Geol Surv Can Bull 417:299–335
Plöchinger B (1955) Zur Geologie des Kalkalpenabschnittes vom Torrener Joch zum Ostfuß des Untersberges; die Göllmasse und die Halleiner Hallstätter Zone. Jb Geol Bundesanst 95:93–144
Plöchinger B (1976) Die Oberalmer Schichten und die Platznahme der Hallstätter Masse in der Zone Hallein-Berchtesgaden, mit Beiträgen von K. Bader und H. Holzer. N Jb Geol Paläont Abh 151:304–324
Plöchinger B (1983) Salzburger Kalkalpen. Samml Geol Führer 73:1–144
Plöchinger B (1984) Zum Nachweis jurassisch-kretazischer Eingleitungen von Hallstätter Gleitmassen beiderseits des Salzach-Quertales (Salzburg). Geol Rundsch 73:293–306
Plöchinger B (1996) Das Halleiner Salinargebiet (Salzburg) im Geotopenschutz-Projekt. Jb Geol Bundesanst 139:497–504
Prey S (1969) Geologische Karte der der Umgebung der Stadt Salzburg 1:50000. Geol Bundesanst
Reading H (1986) Sedimentary environments and facies. Blackwell, Oxford
Reijmer JJG, Everaas SL (1991) Carbonate platform facies reflected in carbonate basin facies (Triassic, Northern Calcareous Alps, Austria). Facies 25:253–278
Reitner J (1997) Stromatolithe und andere Mikrobialithe. In: Steininger F, Maronde D (eds) Städte unter Wasser. Kl Senckenbergr 24:19–37
Reitner J, Gautret P, Marin F, Neuweiler F (1995) Automicrites in a modern marine microbialite. Formation model *via* organic matrices (Lizard Island, Great Barrier Reef, Australia). Bull Inst Océanogr Monaco 14:237–263
Rieche J (1971) Die Hallstätter Kalke der Berchtesgadener Alpen. Unpubl Diss Univ Berlin
Riedel P (1991) Korallen in der Trias der Tethys: Stratigraphische Reichweiten, Diversitätsmuster, Entwicklungstrends und Bedeutung als Rifforganismen. Ges Geol Bergbaustud Österr Mitt 37:97–118
Rüffer T, Zamparelli V (1997) Facies and biota of Anisian to Carnian carbonate platforms in the Northern Calcareous Alps (Tyrol and Bavaria). Facies 37:115–136
Schäfer P, Senowbari-Daryan B (1981) Facies development and paleoecologic zonation of four Upper Triassic patch reefs, Northern Calcareous Alps near Salzburg, Austria. In: Toomey DF (ed) European reef models. SEPM Spec Publ 30:241–259
Schlager W (1969) Das Zusammenwirken von Sedimentation und Bruchtektonik in den triadischen Hallstätterkalken der Ostalpen. Geol Rundsch 59:289–308
Schlager W, Schöllnberger W (1974) Das Prinzip stratigraphischer Wenden in der Schichtenfolge der Nördlichen Kalkalpen. Mitt Geol Ges Wien 66/67:165–193
Schlegel HG (1992) Allgemeine Mikrobiologie. Thieme
Schmidt H (1990) Mikrobohrspuren in Fossilien der triassischen Hallstätter Kalke und ihre bathymetrische Bedeutung. Facies 23:109–120
Schuler G (1968) Lithofazielle, sedimentologische u. paläogeographische Untersuchungen in den Raibler Schichten zwischen Inn und Saalach (Nördliche Kalkalpen). Erlanger Geol Abh 71:1–60
Schulz O (1970) Vergleichende petrographische Untersuchungen an karnischen Sedimenten der Julischen Alpen, Gailtaler Alpen und des Karwendels. Verh Geol Bundesanst 1970:165–229
Schweigl J, Neubauer F (1997) Structural evolution of the central Northern Calcareous Alps: Significance for the Jurassic to Tertiary geodynamics in the Alps. Eclogae Geol Helv 90:303–323
Simms MJ, Ruffel AH (1989) Synchroneity of climate change and extinctions in the Late Triassic. Geology 17:265–268
Stampfli GM, Borel G (2002) Geodynamic evolution of the Alpine Tethys. Internet: http://www-sst.unil.ch/research/plate_tecto/index.htm
Tollmann A (1960) Die Hallstätterzone des östlichen Salzkammergutes und ihr Rahmen. Jb Geol Bundesanst 101:79–115
Tollmann A (1976) Analyse des klassischen nordalpinen Mesozoikums: Stratigraphie, Fauna und Fazies der Nördlichen Kalkalpen. Springer, Berlin Heidelberg New York
Wendt J, Aigner T (1985) Facies patterns and depositional environments of Palaeozoic cephalopod limestones. Sediment Geol 44:263–300
Wilderer PA, Charaklis WG (1989) Structure and function of biofilms. In: Charaklis WG, Wilderer PA (eds) Structure and functions of biofilms. Wiley, pp 5–17